TI Designs
Contactless and Precise AC-Current Sensing Using a Hall Sensor

TI Designs

TI Designs provide the foundation that you need including methodology, testing and design files to quickly evaluate and customize the system. TI Designs help *you* accelerate your time to market.

Design Resources

TIDA–00218	Tool Folder Containing Design Files
DRV5053	Product Folder
MSP430F5529	Product Folder
LP2985–33	Product Folder
TPS7A1633	Product Folder
TMP103	Product Folder
TPD3E001	Product Folder

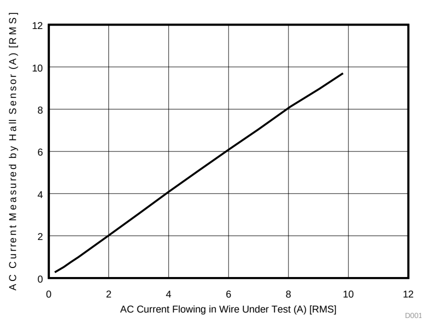

ASK Our E2E Experts
WEBENCH® Calculator Tools

Design Features

This reference design for contactless and precise AC-current sensing using a Hall Sensor subsystem enables AC current measurements while maintaining the insulation around the wire.

- Contactless Proximity Current Sensing for AC, 3-Phase Input Currents
- Maximum Measured Error Less than 5% from 1-A to 10-A RMS
- Flux Concentrator as Described in This Design Improves the Magnetic Flux Density by a Factor of 6 (15 dB)
- Only Single-Point Gain Correction at Maximum Current Range — Second-Order Curve Fit Implemented In Firmware
- Maximum Current that Can Be Sensed Can Be Adapted by Changing Flux Concentrator Design

Featured Applications

- Building Automation
- Circuit Breakers
- Electrical Panels
- Control Panel

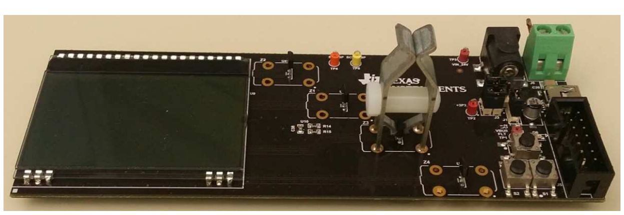

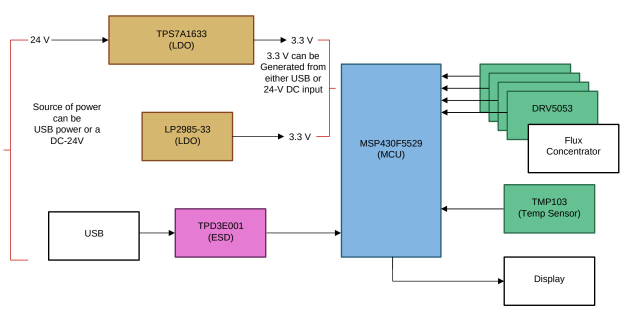

An IMPORTANT NOTICE at the end of this TI reference design addresses authorized use, intellectual property matters and other important disclaimers and information.

Key System Specifications

PARAMETER	SPECIFICATION	DETAILS
Current sensing	Contactless Hall Sensor based, with flux concentrator concentrating the flux	See Section 3.3, Section 3.4, and Section 3.5
Current sensing range	In this design implementation, 500-mA to 10-A AC RMS, however, the maximum current range is dependent on the flux concentrator	See Section 3.4, Section 5.2, and Section 5.3
Flux concentrator material	1010 Cold Rolled Steel (CRS)	See Section 3.5
Input operating voltage	USB powered or 12-V to 24-V DC powered	See Section 4.1 and Section 4.2
Operating temperature	–40 to 85°C	
Cross talk across channels	Negligible	
Temperature effect on Hall Sensor		See Section 5.4
Calibration	Single-point at the maximum current	See Section 3.8.1 and Section 5.1
Maximum measured error	Less than 5%	See Section 5.1
Operating maximum current with this existing flux concentrator design	Approximately 13-A AC RMS	See Section 5.1
Algorithm for current determination	Second-order curve fit that determines current based on Hall Sensor output voltage after gain correction	See Section 5.1
Output	On-board display	See Section 4.1

1 System Description

This reference design for contactless and precise AC-current sensing using a Hall Sensor subsystem provides a solution knowing how much AC current is flowing through a wire without any physical intervention. In some cases during a system debug, determining whether or not an AC current is flowing through the wire is required. The reference design for a contactless AC-current sensing sub-system helps use to do the following:

- Indicate overcurrent alarm conditions
- Determine the load characteristics by monitoring the sourced current
- Indicate alarm conditions when no current is flowing through the monitored wire
- Monitor all three phases of power for debug, data logging or both

The key subsystem challenge during the design process was determining the AC-current flow in a contactless manner. This challenge implies that the plastic insulation around the AC wire is intact yet the user can still determine the AC current flow.

In such a case, one option to determine the AC current flow is to find the magnetic flux around the AC current wire. This method has one challenge that the user must overcome. Even with a high AC current of 10-A flowing through a wire, the magnetic flux generated at the surface is still low, such as 4 Gauss for an 18 gauge wire.

To overcome these challenges, a flux concentrator has been implemented in this subsystem design as shown in Figure 8. The goal of the addition of the flux concentrator, which is non-contact, is to concentrate the flux around the AC current-carrying wire, rather than letting it escape in air, and then direct that flux to a Hall Sensor. Concentrating the magnetic flux using a flux concentrator was improved by more than 15 dB (see Section 3). When this improvement is achieved, then a Hall Sensor and analog output can be used to indicate the strength of the AC current proportional to the Hall Sensor output voltage.

Key Requirements for the Flux Concentrator Design (see Section 3)

- High permeability material
- A design that ensure that the AC current wire is surrounded by this material
- Flexible design so that the ends of the clip can touch the Hall Sensor

Key Requirements for the Hall Sensor

- Use of a through hole package because it provides more flexibility in conjunction with flux concentrator
- An analog output that indicates magnetic-flux concentration

TI's DRV5053 device met the above requirements and was selected for this design (see Section 3).

Key Requirements for the Microcontroller

- ADC input channels
- Enough memory and resources to perform lookup-table functionality as well as linear interpolation

TI's MSP430F5529 device met the above requirements (see Section 3).

1.1 DRV5053

The DRV5053 device is a chopper-stabilized Hall IC that offers a magnetic sensing solution with superior sensitivity stability over temperature and integrated protection features. The 0- to 2-V analog output responds linearly to the applied magnetic flux density and distinguishes the polarity of magnetic flux direction. A wide operating voltage range from 2.5 to 38 V with reverse polarity protection up to –22 V makes the device suitable for a wide range of industrial and consumer applications.

Internal protection functions are provided for reverse supply conditions, load dump, and output short circuit or over current.

1.2 MSP430F5529

The Texas Instruments MSP430™ family of ultralow-power microcontrollers (MCU) consists of several devices featuring different sets of peripherals targeted for various applications. The architecture, combined with extensive low-power modes, is optimized to achieve extended battery life in portable measurement applications. The device features a powerful 16-bit RISC CPU, 16-bit registers, and constant generators that contribute to maximum code efficiency. The digitally controlled oscillator (DCO) allows wake-up from low-power modes to active mode in 3.5 µs (typical).

The MSP430F5529, MSP430F5527, MSP430F5525, and MSP430F5521 devices are microcontroller configurations with integrated USB and PHY supporting USB 2.0, four 16-bit timers, a high-performance 12-bit analog-to-digital converter (ADC), two universal serial communication interfaces (USCI), hardware multiplier, DMA, real-time clock module with alarm capabilities, and 63 I/O pins. The MSP430F5528, MSP430F5526, MSP430F5524, and MSP430F5522 include all of these peripherals but have 47 I/O pins.

The MSP430F5519, MSP430F5517, and MSP430F5515 devices are microcontroller configurations with integrated USB and PHY supporting USB 2.0, four 16-bit timers, two universal serial communication interfaces (USCI), hardware multiplier, DMA, real time clock module with alarm capabilities, and 63 I/O pins. The MSP430F5514 and MSP430FF5513 include all of these peripherals but have 47 I/O pins.

Typical applications include analog and digital sensor systems, data loggers, and others that require connectivity to various USB hosts.

1.3 LP2985–33

The LP2985 family of fixed-output, low-dropout regulators offers exceptional, cost-effective performance for both portable and nonportable applications. Available in voltages of 1.8 V, 2.5 V, 2.8 V, 2.9 V, 3 V, 3.1 V, 3.3 V, 5 V, and 10 V, the family has an output tolerance of 1% for the A version (1.5% for the non-A version) and is capable of delivering 150-mA continuous load current. Standard regulator features, such as overcurrent and overtemperature protection, are included.

The LP2985 device has a host of features that makes the regulator an ideal candidate for a variety of portable applications. These features include the following:

- Low dropout: A PNP pass element allows a typical dropout of 280 mV at 150-mA load current and 7 mV at 1-mA load.
- Low quiescent current: The use of a vertical PNP process allows for quiescent currents that are considerably lower than those associated with traditional lateral PNP regulators
- Low dropout: A PNP pass element allows a typical dropout of 280 mV at 150-mA load current and 7 mV at 1-mA load.

- Low quiescent current: The use of a vertical PNP process allows for quiescent currents that are considerably lower than those associated with traditional lateral PNP regulators
- Shutdown: A shutdown feature is available, allowing the regulator to consume only 0.01 μA when the ON/OFF pin is pulled low.
- Low-ESR-capacitor friendly: The regulator is stable with low-ESR capacitors, allowing the use of small, inexpensive, ceramic capacitors in cost-sensitive applications.
- Low noise: A BYPASS pin allows for low-noise operation, with a typical output noise of 30 μVRMS, with the use of a 10-nF bypass capacitor.
- Small packaging: For the most space-constrained needs, the regulator is available in the SOT–23 package.

1.4 TPS7A1633

The TPS7A16 family of ultralow power, low-dropout (LDO) voltage regulators offers the benefits of ultra-low quiescent current, high input voltage, and miniaturized, high thermal-performance packaging. The TPS7A16 family of devices is designed for continuous or sporadic (power backup) battery-powered applications where ultra-low quiescent current is critical to extending system battery life. The TPS7A16 family offers an enable pin (EN) compatible with standard CMOS logic and an integrated open drain active-high power good output (PG) with a user programmable delay. These pins are intended for use in microcontroller-based, battery powered applications where power-rail sequencing is required. In addition, the TPS7A16 is ideal for generating a low-voltage supply from multicell solutions ranging from high cell-count power-tool packs to automotive applications; not only can this device supply a well-regulated voltage rail, but it can also withstand and maintain regulation during voltage transients. These features translate to simpler and more cost-effective, electrical surge-protection circuitry.

1.5 TMP103

The TMP103 device is a digital-output temperature sensor in a four-ball wafer chip-scale package (WCSP). The TMP103 device is capable of reading temperatures to a resolution of 1°C. The TMP103 device features a two-wire interface that is compatible with both I^2C and SMBus interfaces. In addition, the interface supports multiple device access (MDA) commands that allow the master to communicate with multiple devices on the bus simultaneously, eliminating the need to send individual commands to each TMP103 device on the bus. Up to eight TMP103 devices can be tied together in parallel and easily read by the host. The TMP103 device is especially ideal for space-constrained, power-sensitive applications with multiple temperature measurement zones that must be monitored. The TMP103 device is specified for operation over a temperature range of –40°C to 125°C.

1.6 TPD3E001

The TPD3E001 is a low-capacitance ±15-kV ESD-protection diode array designed to protect sensitive electronics attached to communication lines. Each channel consists of a pair of diodes that steer ESD current pulses to V_{CC} or GND. The TPD3E001 device protects against ESD pulses up to ±15-kV human-body model (HBM), ±8-kV contact discharge, and ±15-kV air-gap discharge, as specified in IEC 61000–4–2. This device has a 1.5-pF capacitance per channel, making it ideal for use in high-speed data IO interfaces.

The TPD3E001 device is a triple-ESD structure designed for USB On-the-Go (OTG) and video applications.

The TPD3E001 device is available in DRL, DRY, and thin QFN packages and is specified for –40°C to 85°C operation.

2 Block Diagram

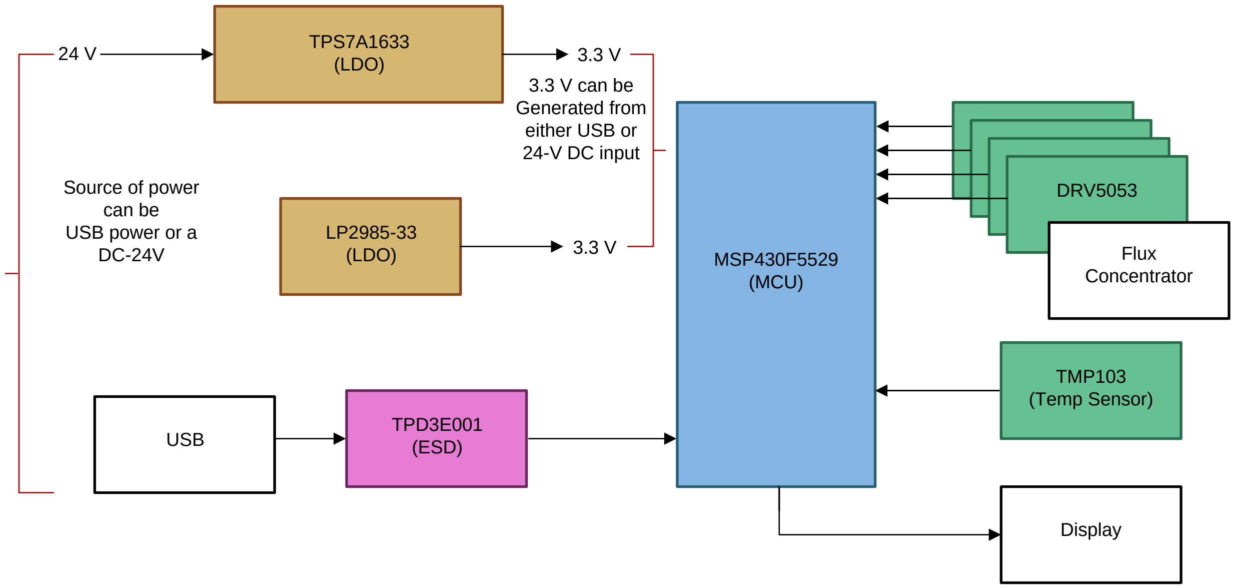

Figure 1. Contactless and Precise AC Current Sensing Using Hall Sensor Block Diagram

2.1 Highlighted Products

The reference design for contactless and precise AC-current sensing using a Hall Sensor features the following devices:

- DRV5053
  - 2.5-V to 38-V analog-bipolar, hall-effect sensor
- MSP430F5529
  - 16-bit ultralow power microcontroller, 128-kB flash, 8-kB RAM, USB, 12-bit ADC, 2 USCIs, 32-bit HW MPY
- LP2985–33
  - Single output LDO, 150 mA, fixed (3.3 V), 1.5% tolerance, low quiescent current, low noise
- TPS7A1633
  - 60-V, 5-µA I_Q, low-dropout 100-mA linear regulator with enable and power good
- TMP103
  - Digital temperature sensor with I^2C and SMBUS expanded interface
- TPD3E001
  - Low-capacitance 3-channel ±15KV ESD-protection array for high-speed data interfaces

For more information on each of these devices, see the respective product folders at www.ti.com or the resources listed in Section 7.

2.1.1 DRV5053

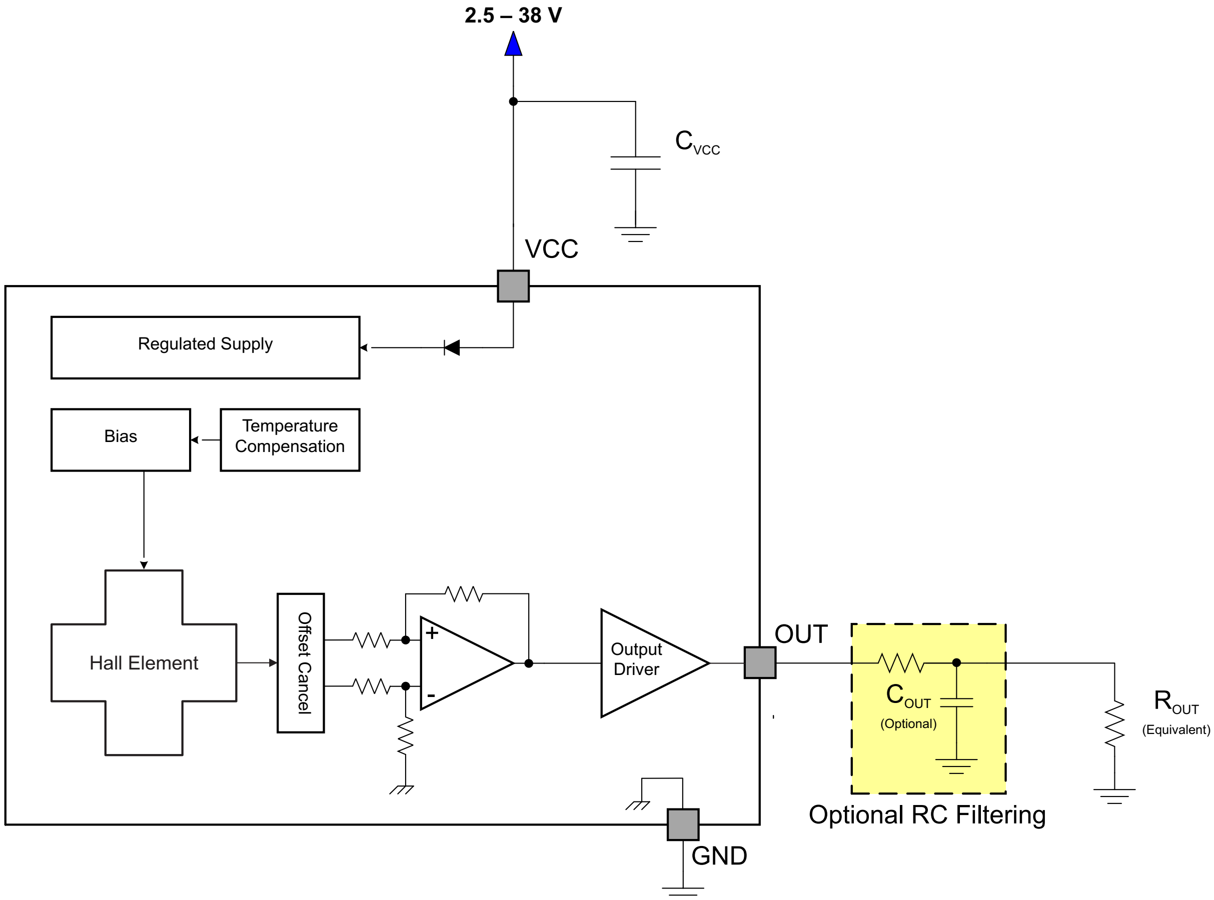

Figure 2. DRV5053 Functional Block Diagram

The DRV5053 features are as follows:

- Linear output Hall Sensor
- Superior temperature stability
  - Sensitivity ±10% over temperature
- High sensitivity options:
  - –11 mV/mT (OA)
  - –23 mV/mT (PA)
  - –45 mV/mT (RA)
  - –90 mV/mT (VA)
  - +23 mV/mT (CA)
  - +45 mV/mT (EA)
- Supports a wide voltage range
  - 2.5 to 38 V
  - No external regulator required
- Wide operating temperature range
  - T_A = –40 to 125°C (Q)
- Amplified output stage
  - 2.3-mA sink, 300 µA source
- Output voltage: 0.2 ~ 1.8 V

  - B = 0 mT, OUT = 1 V
- Fast power-on: 35 µs
- Small package and footprint
  - Surface mount 3-Pin SOT–23 (DBZ)
    - 2.92 mm × 2.37 mm
  - Through-hole 3-pin SIP (LPG)
    - 4 mm × 3.15 mm
- **Protection features:**
  - Reverse supply protection (up to –22 V)
  - Supports up to 40-V load dump
  - Output short-circuit protection
  - Output current limitation

2.1.2 MSP430F5529

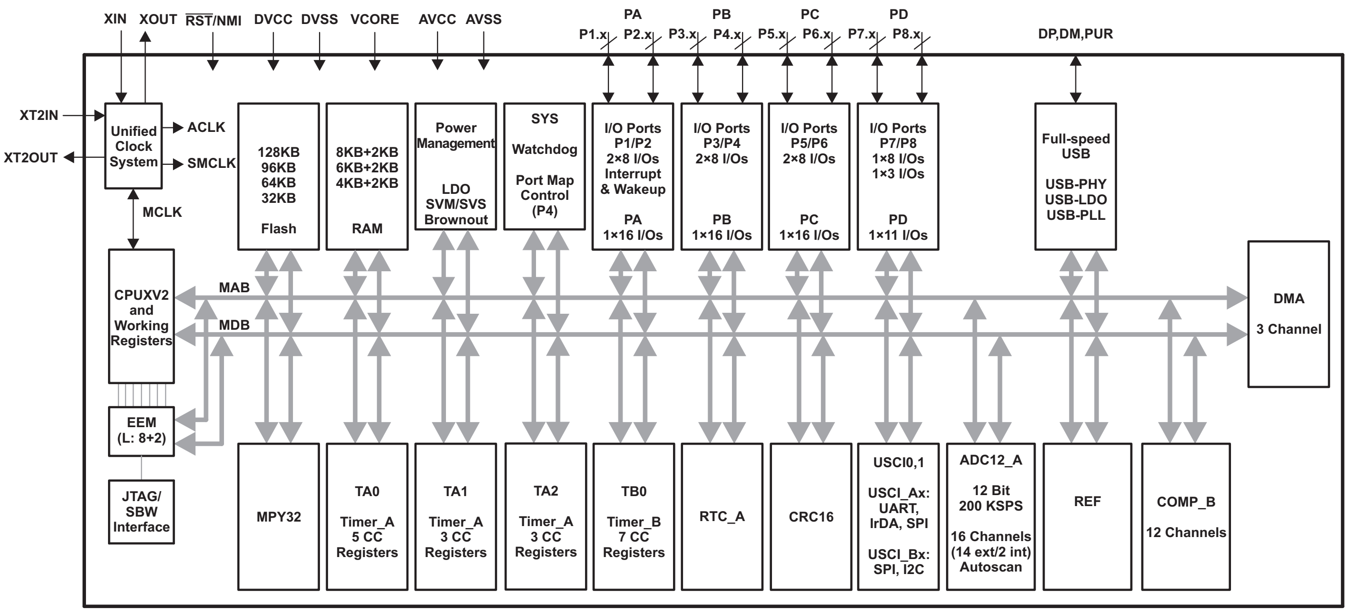

Figure 3. MSP430F5529 Functional Block Diagram

The MSP430F5529 features are as follows:

- Low supply-voltage range: 3.6 V down to 1.8 V
- Ultralow-power consumption
  - Active mode (AM): all system clocks active 290 µA/MHz at 8 MHz, 3, flash program execution (Typical) 150 µA/MHz at 8 MHz, 3, RAM program execution (typical)
  - Standby mode (LPM3): real-time clock with crystal, watchdog, and supply supervisor operational, full RAM retention, Fast Wake-Up: 1.9 µA at 2.2 V, 2.1 µA at 3 (typical) low-power oscillator (VLO), general-purpose counter, watchdog, and supply supervisor operational, full RAM retention, fast wake up: 1.4 µA at 3 (typical)
  - Off mode (LPM4): full RAM retention, supply supervisor operational, fast wake up: 1.1 µA at 3 V (typical)
  - Shutdown mode (LPM4.5): 0.18 µA at 3 (Typical)
- Wake up from standby mode in 3.5 µs (typical)
- 16-bit RISC architecture, extended memory, up to 25-MHz system clock
- Flexible power management system

- Fully integrated LDO with programmable regulated core supply voltage
- Supply voltage supervision, monitoring, and brownout

- Unified clock system
  - FLL control loop for frequency stabilization
  - Low-power low-frequency internal clock source (VLO)
  - Low-frequency trimmed internal reference source (REFO)
  - 32-kHz watch crystals (XT1)
  - High-frequency crystals up to 32 MHz (XT2)
- 16-bit timer TA0, Timer_A with five capture and compare registers
- 16-bit timer TA1, Timer_A with three capture and compare Registers
- 16-bit timer TA2, Timer_A with three capture and compare Registers
- 16-bit timer TB0, Timer_B with seven capture and compare shadow registers
- Two universal serial communication interfaces
  - USCI_A0 and USCI_A1 each support:
    - Enhanced UART supports auto-baudrate detection
    - IrDA encoder and decoder
    - Synchronous SPI
  - USCI_B0 and USCI_B1 each support:
    - I^2C
    - Synchronous SPI
- Full-speed universal serial bus (USB)
  - Integrated USB-PHY
  - Integrated 3.3-V and 1.8-V USB power system
  - Integrated USB-PLL
  - Eight input and eight output endpoints
- 12-Bit analog-to-digital converter (ADC) (MSP430F552x only) with internal reference, sample-and-hold, and autoscan feature
- Comparator
- Hardware multiplier supports 32-bit operations
- Serial onboard programming, no external programming voltage needed
- Three-channel internal DMA
- Basic timer with real-time clock feature
- See the data sheet for a list of devices in this device family, SLAS590
- For complete module descriptions, see the *MSP430x5xx and MSP430x6xx Family User's Guide*, SLAU208

2.1.3 LP2985–33

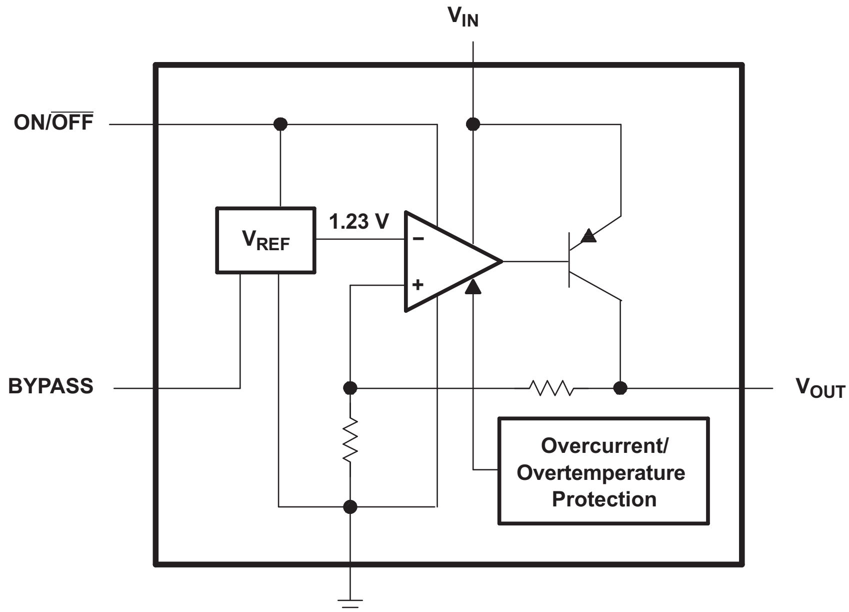

Figure 4. LP2985 Functional Block Diagram

The LP295 features are as follows:

- Output tolerance of
  - 1% (A grade)
  - 1.5% (standard grade)
- Ultralow dropout, typically
  - 280 mV at full load of 150 mA
  - 7 mV at 1 mA
- Wide V_{IN} range: 16 V maximum
- Low I_Q: 850 µA at full load at 150 mA
- Shutdown current: 0.01 µA typical
- Low noise: 30 μV_{RMS} with 10-nF bypass capacitor
- Stable with low-ESR capacitors, including ceramic
- Overcurrent and thermal protection
- High peak-current capability
- ESD protection exceeds JESD 22
  - 2000-V human-body model (A114-A)
  - 200-V machine model (A115-A)

2.1.4 TPS7A1633

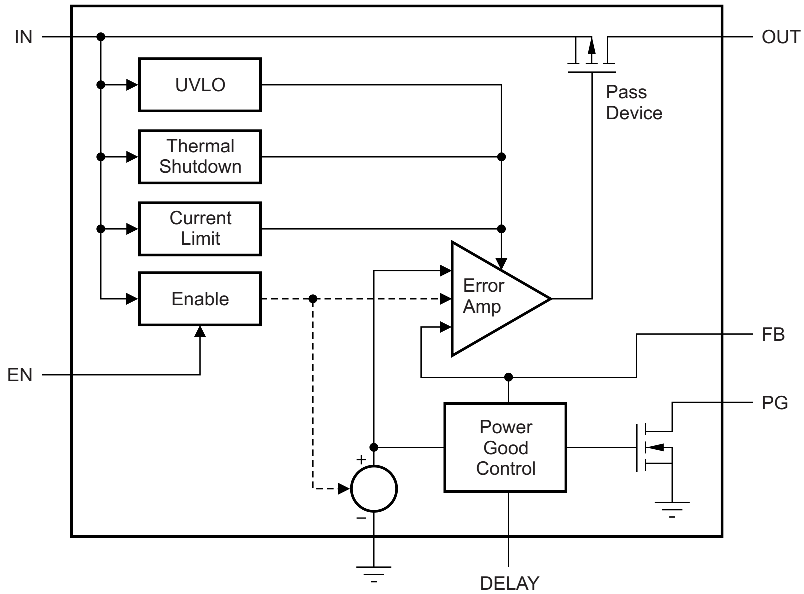

Figure 5. TPS7A1633 Functional Block Diagram

The TPS7A1633 features are as follows:

- Wide input voltage range: 3 to 60 V
- Ultralow quiescent current: 5 µA
- Quiescent current at shutdown: 1 µA
- Output current: 100 mA
- Low dropout voltage: 60 mV at 20 mA
- Accuracy: 2%
- Available in:
  - Fixed output voltage: 3.3 V, 5 V
  - Adjustable version from 1.2 to 18.5 V
- Power good with programmable delay
- Current-limit and thermal shutdown protections
- Stable with ceramic output capacitors: ≥ 2.2 µF
- Packages: high thermal performance MSOP–8 and SON–8 PowerPAD™
- Operating temperature range: –40°C to 125°C

2.1.5 TMP103

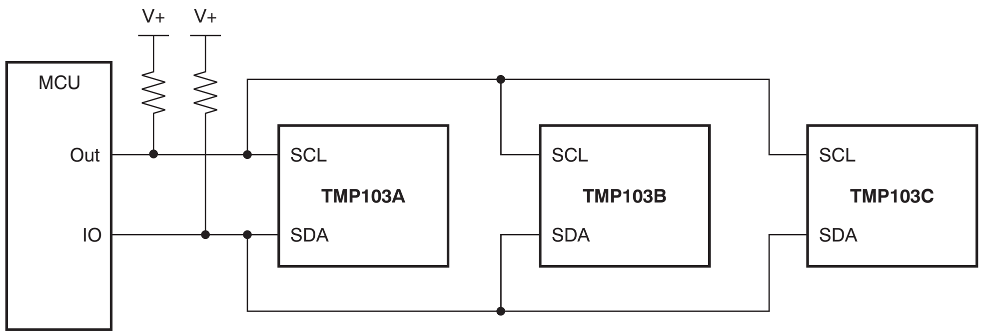

Figure 6. TMP103 Pin Configuration

The TMP103 features are as follows:

- Multiple device access (MDA):
  - Global read and write operations
- I^2C- and SMBus™-compatible interface
- Resolution: 8 bits
- Accuracy: ±1°C typical (–10°C to 100°C)
- Low quiescent current:
  - 3-µA active I_Q current at 0.25Hz
  - 1-µA shutdown current
- Supply range: 1.4 to 3.6 V
- Digital output
- Package: 4-Ball WCSP (DSBGA)

2.1.6 TPD3E001

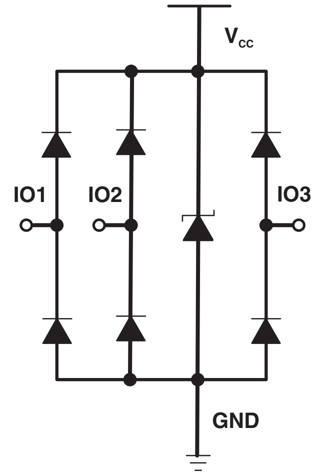

Figure 7. TPD3E001 Logic Block Diagram

The TPD3E001 features are as follows:

- 3-Channel ESD clamp array to enhance system-level ESD protection
- Exceeds IEC61000–4–2 (level–4) ESD protection requirements
  - ±8-kV IEC 61000–4–2 contact discharge
  - ±15-kV IEC 61000–4–2 air-gap discharge
- ±15-kV human-body model (HBM)
- 5.5-A peak pulse current (8/20-μs Pulse)
- Low 1.5-pF input-output capacitance
- Low 1-nA (max) leakage current
- 0.9- to 5.5-V supply-voltage range
- Space saving DRY, DRL, and DRS package options
- Alternate 2-, 4-, and 6-channel options available: TPD2E001, TPD4E001, and TPD6E001

3 System Design Theory

3.1 Magnetic Field

The magnetic field lines around a long wire carrying an electric current form concentric circles around the wire. The direction of the magnetic field is perpendicular to the wire and the direction of the current flow follows the right-hand rule. When the user wraps their right hand around the wire with their fingers curling in the direction of the magnetic field, the direction of the pointing thumb is the direction of the current flow. The magnetic field of an infinitely-long straight wire can be obtained by applying Ampere's law. The expression for the magnetic field is shown in Equation 1.

$$B = \frac{\mu \times I}{2 \times \pi \times r} \quad (1)$$

where

- B = magnetic field
- I = current in Amperes
- R = radial distance in m
- μ = permeability in free space: $4\pi 10^{-7}$ T.m/A

As shown in Equation 1, the magnetic energy generated by a current-carrying wire is low even at 10 A for an 18-AWG wire. The magnetic field is only 4 Gauss.

3.2 Permeability

Permeability is the degree of magnetization the material gains as a response to that field. Permeability occurs when a magnetic field is applied to a material.

Using the information in Section 3.1 and this section, concentrating the magnetic flux from the AC current-carrying wire is desirable such that a wider dynamic-range response can be obtained from the Hall Sensor output that is indicative of the AC current.

3.3 Flux Concentrator

Multiple ferrite cores were shaped in a form as shown in Figure 8. The purpose of this form is to force the AC current-carrying wire through the opening in the flux concentrator such that the flux concentrator surrounds the AC current-carrying wire. Then, as the flux concentrator tapers it can direct the magnetic flux through the through-hole package on the Hall Sensor DRV5053 device.

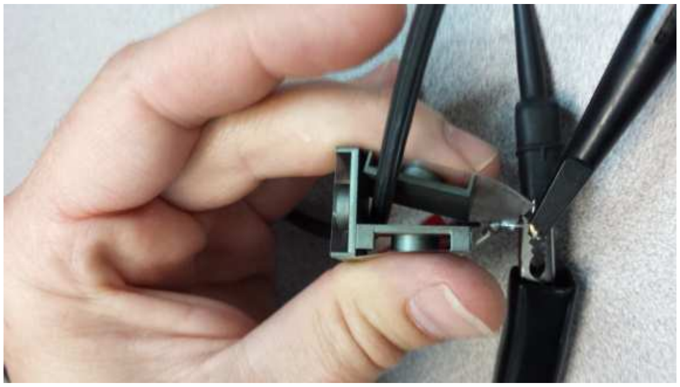

Figure 8. Flux Concentrator Concept

3.4 AC Current Magnetic Flux With and Without Flux Concentrator

This section shows the improvement received by using a flux concentrator versus not using a flux concentrator. The results were generated using the following steps:

- Use a space heater for a resistive load. Feed the current from the cord of the heater (AC line) through the flux concentrator as shown in Figure 8.
- Use a space heater for a lower setting (the equivalent of 6.8-A was measured on the power meter) and as shown in Figure 9.

  The Hall Effect sensor measured 272 mV_{PP}.
- To confirm if the flux concentrator had an effect, use the same current and remove the flux concentrator. Place the hall effect sensor next to the cord.

  Figure 10 shows the results. The peak-to-peak (pp) amplitude was measured at only 46 mV.

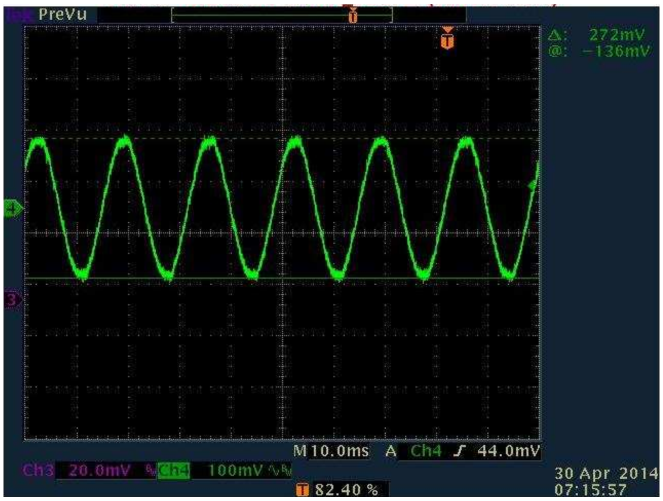

Figure 9. With Flux Concentrator

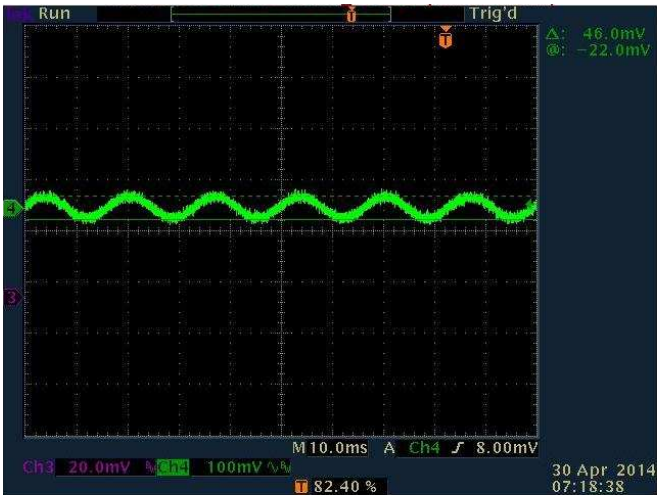

Figure 10. Without Flux Concentrator

The results confirmed that a first attempt at designing a flux concentrator resulted in an improved magnetic flux of approximately 15 dB. This result can translate into a more accurate response for the Hall Sensor DRV5053 device over a wide dynamic range of AC currents.

3.5 Flux Concentrator Design

A detailed CAD drawing was generated such that a flux concentrator can be manufactured to given tolerances as shown in Figure 11 and Figure 12. The flux concentrator was designed using 1010 CRS material.

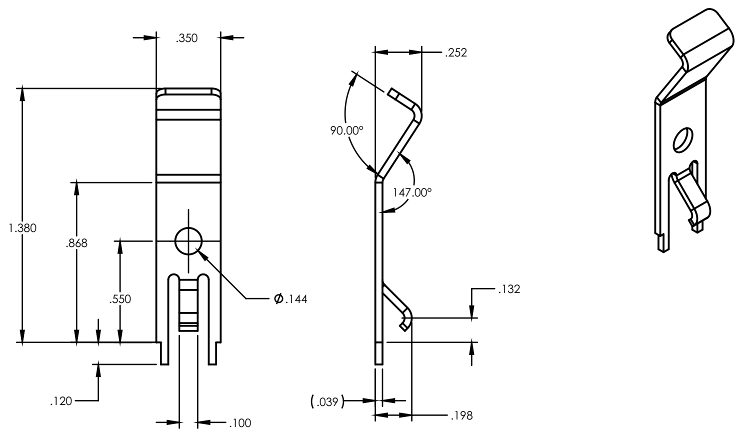

Dimensions are in Inches.

Figure 11. Flux Concentrator Drawing

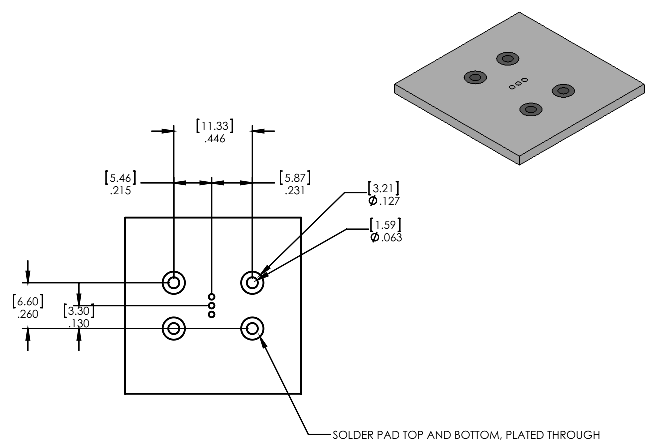

Dimensions are in Inches.

Figure 12. Flux Concentrator Solder Pads for PCB

3.6 Low-Pass Filter on DRV5053 Analog Outputs

The output bandwidth of the DRV5053 device is 20 kHz. The AC current under measurement is 60 Hz. A low-pass filter was included on the DRV5053 outputs so that the cutoff frequency is 225 Hz. The intent of the low-pass filter is to filter the high frequency noise from the analog output lines of DRV5053 device above 3 to 4 times the frequency of interest, which, in this case, is 60 Hz.

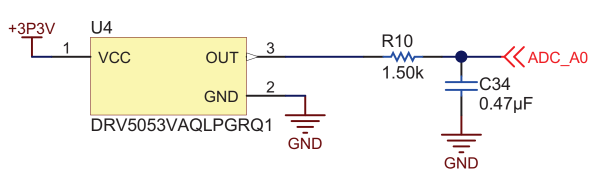

Figure 13. Low-Pass Filter on DRV5053 Analog Outputs

3.7 DRV5053 Analog Lines Layout

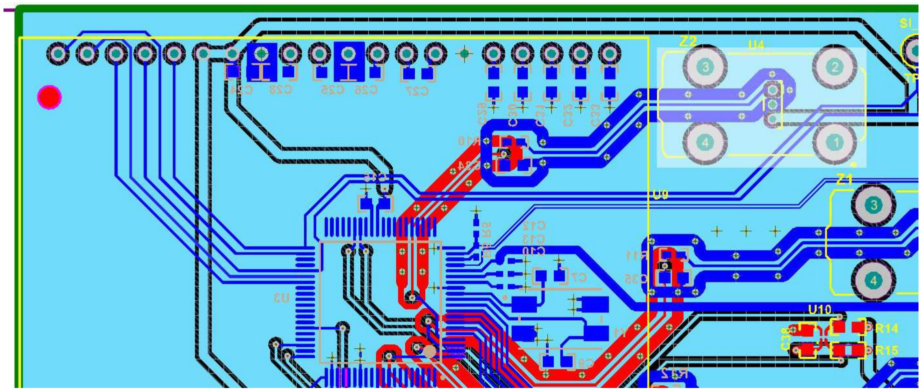

Figure 14. DRV5053 Analog Output Layout

The design guidelines for the analog layout were followed for the DRV5053 analog output. As shown in Figure 14, the analog output line was surrounded by ground pours with via stitching such that the noise from any surrounding circuitry or other source can be isolated from the analog output lines.

The low-pass filter was placed closer to the MSP430 ADC input pins.

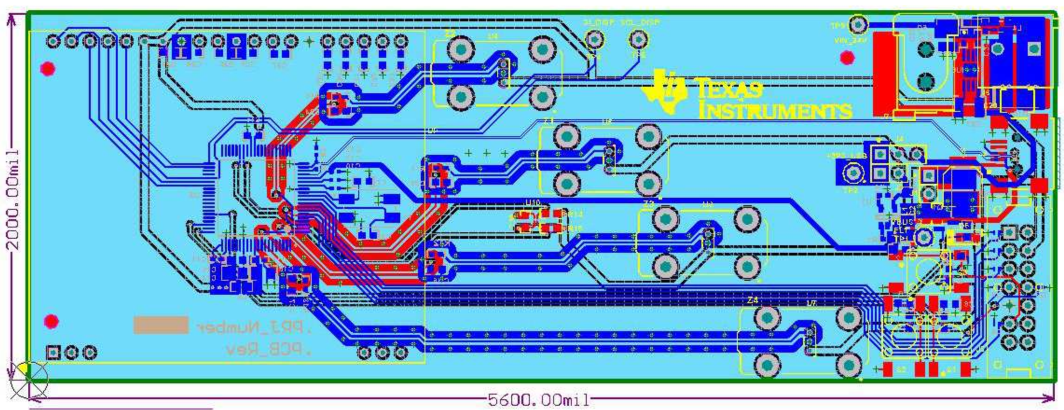

Figure 15. Flux Concentrator, Hall Sensor Placement With Respect to Input Power

The Hall Sensor was placed directly underneath the flux concentrator and away from the power and EP section as shown in Figure 15.

3.8 MSP430 ADC Resources

The MSP430F5529 device has an internal 12-bit successive approximation (SAR) analog-to-digital converter (ADC). The internal ADC samples the DRV5053 device on each channel. Use to calculate the ADC count value based on the actual voltage signal from the DRV5053 device.

ADC count = (3.3 V × sample) / 4095

The external reference voltage of the ADC is set to 3.3 V as shown in Figure 13. The value 4095 is used because the internal ADC has 12-bits of accuracy, $2^{12} = 4096$.

3.8.1 Firmware Description

The three main clocks, ACLK, SMCLK, and MCLK, are referenced off of the external 24-MHz crystal. The ACLK clock oscillates at 3 MHz, the SMCLK clock oscillates at 6 Mhz, and the MCLK clock oscillates at 24 MHz. An open-source TI library, IQMath, calculates the RMS value for the user in a time-efficient matter. To download the IQMath library, go to www.ti.com/tool/msp430-iqmathlib.

A calibration sequence runs on startup and requires 2 s of data to find the average noise. The average noise value is removed from each sample before adding it to the total run time.

When the ADC is configured with the respective buffers and a sampling rate of approximately 5940 samples per second, the calibration is complete. The main loop waits until the sample buffer completes a full second of data (5940 samples). The ADC triggers an interrupt when a sample can be read. At this time, the sample is squared and added to a running total. After 5940 samples are taken, the running total is copied to another buffer. The previous total is cleared and the ADC is ready to receive new data. While waiting for more ADC interrupts, RMS calculations can occur with the new buffer as shown in Equation 2.

$$\mathrm{RMS} = \sqrt{\frac{1}{n}\Sigma_n x^2} \tag{2}$$

Because the sum of squares are already calculated with the running total, only the divide and square root must be calculated. Peak-to-peak values are stored during the sampling stage of ADC interrupt-service routine and are updated every second along with the calculated RMS and current values.

4 Hardware Overview

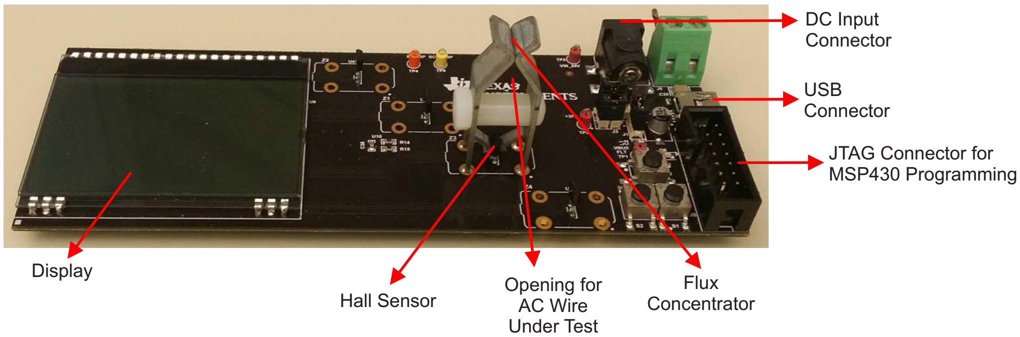

Figure 16. Hardware Description

4.1 USB Power

To set up the USB power, follow these steps:

- Install jumper J1 and J3.
- Ensure that the J4 jumper is installed between pins 1 and 2.

  The default of the firmware is set to a value so that the threshold for the RMS-voltage readout from the analog output of the DRV5053 device is 15 mV. This default value means that as long as the noise on the lines is below 15 mV, the design will read 0 A of current.
- Pass current-carrying wire under test through the opening in the flux concentrator as shown in Figure 21.
- Ensure that the plastic insulation on the AC wire is intact.

  The MSP430 firmware performs a running average of the sample size. The sample frequency is approximately 5940 samples per second. The display is updated about every second after the RMS calculations are complete.

  See Figure 17 for the display readout description.

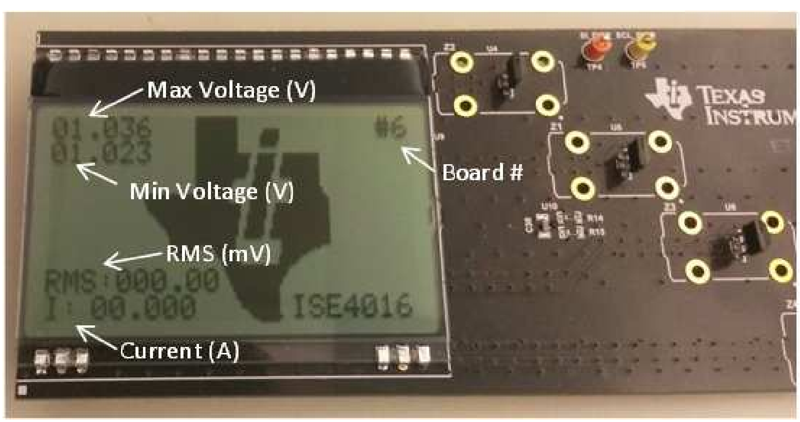

Figure 17. Display Readout Description

4.2 24-V DC Power Source

To set up the 24-V DC power source, follow these steps:

- Install jumper J1 and J3.
- Ensure that the J4 jumper is installed between pins 2 and 3.
- See Section 4.1 for the remaining steps.

5 Test Data

5.1 Maximum Measured Error

Figure 18. Power Source

A Kikusui PCR1000M power source was used to source the variable AC currents. The AC voltage was kept low for safety reasons and to ensure that the power across resistor loads was kept low.

Figure 19. Power Meter

A Voltek PM1000+ power meter was made available if needed. However, for this test, the use of a current probe was needed for data logging purposes. The corresponding AC peak-to-peak, RMS readings, and the Hall voltage output was recorded across different settings.

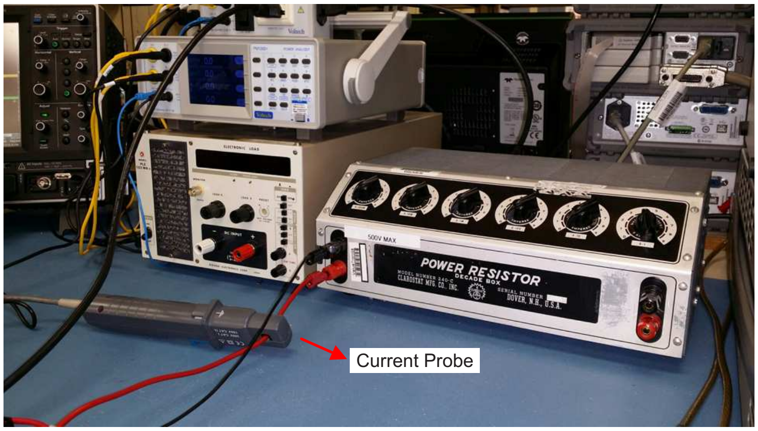

Figure 20. Hardware Description

A Clarostat decade box was used as a resistive load across different AC input-current settings.

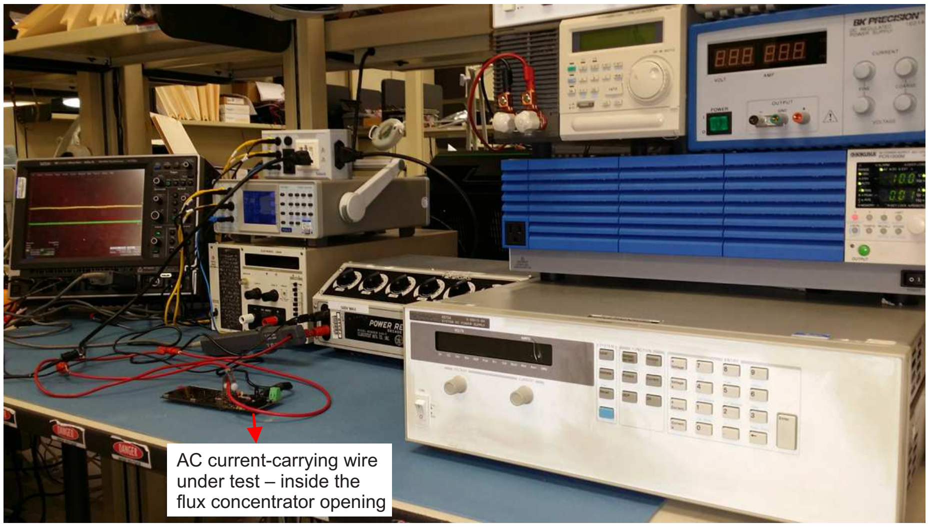

Figure 21. Complete Setup

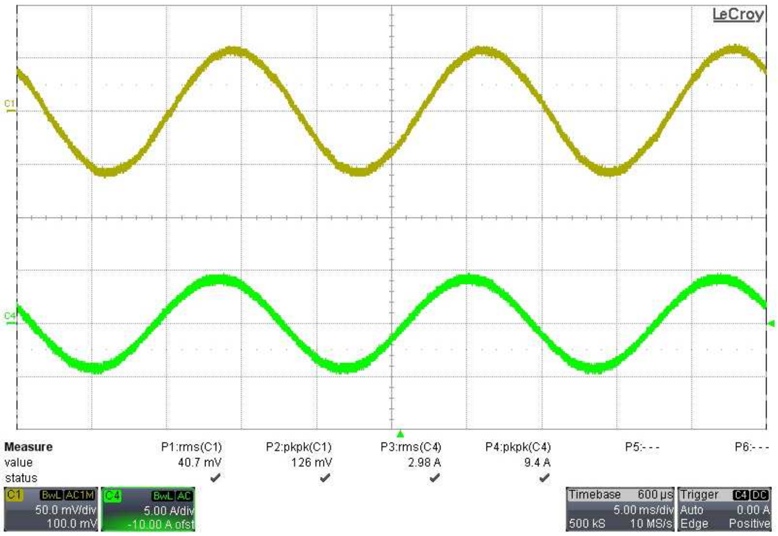

Figure 22. AC Current Probe Measurement and Hall Sensor Output Voltage

Measurements of the Hall Sensor output voltage were taken across different AC current settings as shown in Figure 22 . Table 1 lists the RMS and pp values for the AC input current and the Hall Sensor output voltage for each measurement.

Table 1. Sensor Output Voltage Across Different AC input Currents

TEMP.	BOARD 5				BOARD 6 (1)				BOARD 7			
	CURRENT FLOWING IN WIRE		HALL SENSOR MEASUREMENT		CURRENT FLOWING IN WIRE		HALL SENSOR MEASUREMENT		CURRENT FLOWING IN WIRE		HALL SENSOR MEASUREMENT	
°C	pp (A)	RMS (A)	pp (mV)	RMS (mV)	pp (A)	RMS (A)	pp (mV)	RMS (mV)	pp (A)	RMS (A)	pp (mV)	RMS (mV)
Room	0.66	0.2	14.1	2.53	0.66	0.2	16.6	3.42	0.69	0.2	14.1	2.92
Room	1.6	0.49	24.3	5.94	1.63	0.5	29.4	7.78	1.63	0.5	27.5	7
Room	2.34	0.75	32	9.26	2.34	0.75	39.7	11.77	2.37	0.75	35.8	10.88
Room	3.04	1	42.2	12.54	3.01	0.99	51.2	15.61	3.01	1	53	14.6
Room	6.02	2	85	26.2	6.14	2.04	115	33.8	6.08	2	96	29.9
Room	9.4	2.98	126	40.7	9.4	3.01	166	51.9	9.4	3.01	146	47.1
Room	12.3	4.01	174	57.5	12.3	4	224	71.7	12.3	3.99	205	65.3
Room	15	4.96	227	73.9	15	4.98	282	92.3	15.2	5	259	84.4
Room	21.8	6.98	330	109.3	21.8	6.99	429	138.4	21.8	6.99	371	124.5
Room	30.4	10.0	506	166.6	30.1	9.95	634	210.8	30.4	9.98	570	189.3

(1) Board 6 was used as the baseline for the curve fit and gain error correction.

As listed in Table 1, for this particular set of data collection, a maximum current of 10 A was used (limited by the test equipment). The maximum current measured was not limited by the Hall Sensor capability (see Section 5.2).

To calibrate the Hall Sensor across different systems, a single-point gain calibration is proposed.

In this setup, the gain calibration of 10 A was used across board 5 and board 7 for gain correction with board 6 as the baseline. Figure 23 shows a second-order polynomial.

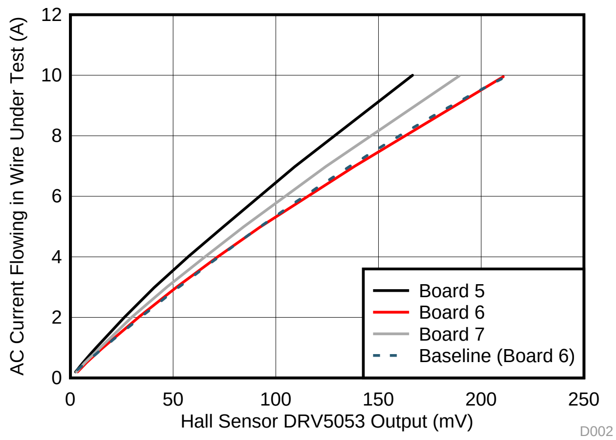

$y = -0.0000554x^2 + 0.0583711x + 0.0712513$, $R^2 = 0.9997402$

Figure 23. Hall Sensor Output Response Across Different Boards and Curve Fit

Table 2. Measured Error of Board 5 After Gain Calibration and Curve Fit Equation of Board 6 as Reference

BOARD 5 HALL SENSOR MEASUREMENT			
GAIN CORRECTED HALL SENSOR OUTPUT VOLTAGE (mV)	REFERENCE CURRENT FLOWING IN WIRE RMS (A)	2ND ORDER CURVE FIT TO PREDICT CURRENT (A)	ERROR
3.22	0.2	0.26	29.24%
7.55	0.49	0.51	3.67%
11.78	0.75	0.75	0.01%
15.95	1	0.99	1.5%
33.32	2	1.95	2.03%
51.76	2.98	2.94	1.21%
73.12	4.01	4.04	0.83%
93.98	4.96	5.07	2.17%
138.99	6.98	7.11	1.92%
211.86	10	9.95	0.49%

As shown in Table 2, the measured error on board 5 is only 2.17% from 1 A to 10 A with board 6 curve fit equation and after gain calibration.

Table 3. Measured Error of Board 7 After Gain Calibration and Curve Fit Equation of Board 6 as Reference

BOARD 7 HALL SENSOR MEASUREMENT			
GAIN CORRECTED HALL SENSOR OUTPUT VOLTAGE (mV)	REFERENCE CURRENT FLOWING IN WIRE RMS (A)	2ND ORDER CURVE FIT TO PREDICT CURRENT (A)	ERROR
3.26	0.2	0.26	30.52%
7.82	0.49	0.52	4.85%
12.15	0.75	0.77	2.71%
16.31	1	1.01	0.64%
33.4	2	1.96	2.2%
52.61	2.98	2.99	0.71%
72.94	4.01	4.03	1.1%
94.27	4.96	5.08	1.63%
139.06	6.98	7.12	1.82%
211.44	10	9.94	0.44%

As shown in Table 3, the measured error on board 7 is only 2.2% from 1 A to 10 A using board 6 curve fit equation and after gain calibration.

The equation used to calculate current from the RMS value was adjusted to allow for current measurement down to 0.5 A.

In this setup, measurements were taken from 0.5 A to 10 A using board 7. Figure 24 shows a second-order polynomial fit.

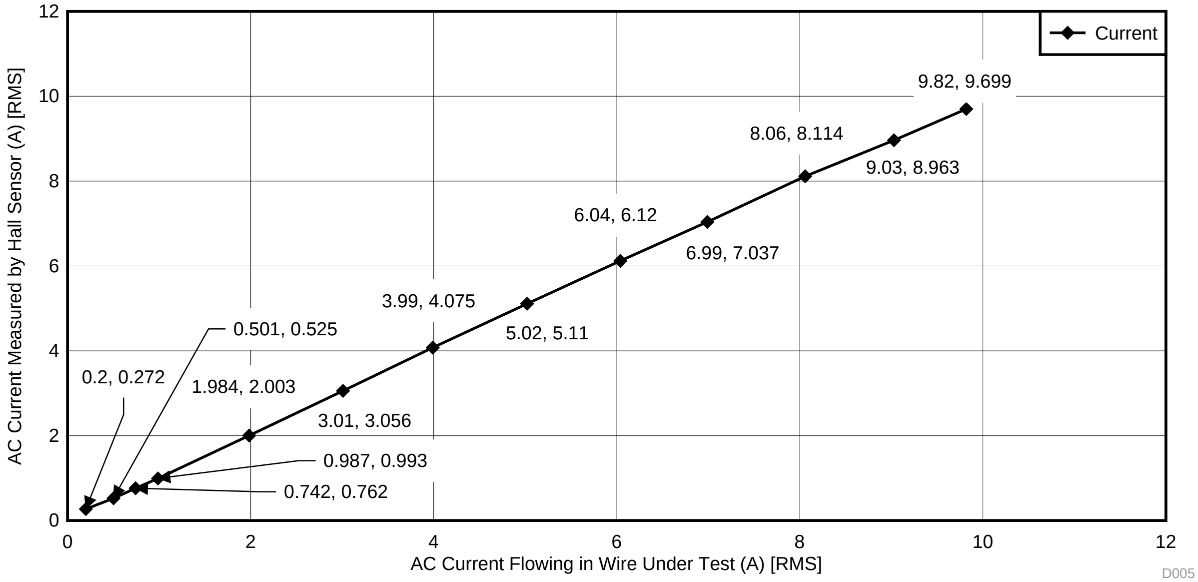

Figure 24. Hall Sensor Response to AC Current Flowing in a Wire from 0.5 A to 10 A

Table 4. Board 7 After Curve Fit from 0.5 A to 10 A

BOARD 7 HALL SENSOR MEASUREMENT		
REFERENCE CURRENT FLOWING IN WIRE (A)	HALL SENSOR 2ND ORDER CURVE FIT TO PREDICT CURRENT (A)	ERROR
0.2	0.272	–36%
0.501	0.525	–5%
0.742	0.762	–3%
0.987	0.993	–1%
1.984	2.003	–1%
3.01	3.056	–2%
3.99	4.075	–2%
5.02	5.11	–2%
6.04	6.12	–1%
6.99	7.037	–1%
8.06	8.114	–1%
9.03	8.963	1%
9.82	9.699	1%

As listed in Table 4, the measured error on board 7 is within 5% of the actual AC current through the wire from 1 A to 10 A.

5.2 Maximum Current Range

To ensure that the Hall Sensor output is not saturated, putting the maximum current specification that the system can sense based on the overall sensitivity specification of the Hall Sensor is important.

For the DRV5053 device the sensitivity is from –140 mV/mT to –35 mV/mT based on the device data sheet.

To ensure that the output is not saturated at the maximum current across the device range, use the known B field versus output voltage of the Hall Sensor data that was collected on a unit (referred here as calibrated unit) as listed in Table 5 .

Table 5. Sensitivity Data Across Known B Field

MAGNETIC FIELD (B) MEASURED	HALL SENSOR OUTPUT VOLTAGE	SENSITIVITY
+0 mT	1.003 V	
+0.55 mT	1.05 V	
+1.15 mT	1.102 V	–86.7 mV/mT
+1.75 mT	1.15 V	–80 mV/mT
+2.37 mT	1.2 V	–80.6 mV/mT
+2.98 mT	1.252 V	–85.2 mV/mT
+4.5 mT	1.375 V	–80.9 mV/mT
+6 mT	1.5 V	–83.3 mV/mT
+7.53 mT	1.624 V	–81 mV/mT
+9.03 mT	1.749 V	–83.3 mV/mT

This particular unit was then soldered on board 7and, with the same setup (see Section 5.1) , data was collected across different known currents as listed in Table 6.

Table 6. Output Voltage versus AC Current

TEMPERATURE	BOARD 7 WITH CALIBRATED UNIT SOLDERED			
	CURRENT FLOWING IN WIRE		HALL SENSOR MEASUREMENT	
°C	pp (A)	RMS (A)	pp (mV)	RMS (mV)
Room	1.5	0.5	33.3	7.24
Room	3.04	1	58	14.5
Room	6.08	2.01	101	30.5
Room	9.4	2.99	152	47.8
Room	12.5	4.02	211	65.8
Room	15.2	5.01	262	84.9
Room	21.8	7	390	124.7
Room	30.4	10.01	582	191.9

As listed in Table 6, the pp range for the 10-A range is 582 mV. As listed in Table 5, this value corresponds to approximately +7 mT in the mT range.

Assuming the worst case with a device that has sensitivity of –140mV/mT, then the overall mT range is approximately +10 mT, assuming a total V_{OUT} range of 1.4 V for the Hall Sensor (assuming a V_{OUT} common mode of 1.1 V and maximum pp of 1.8 V}.

Therefore, in a worst-case scenario with a device sensitivity of –140mV/mT, the maximum current that can be sensed with this existing flux concentrator design is approximately 14 A before saturation.

However ,the flux concentrator design can easily be changed (either the material or design) to increase the maximum current range if desired.

5.3 Minimum Current Range

The minimum current of the system is determined by the noise of the Hall Sensor output under quiescent conditions. As previously stated, a low-pass filter is included in this design to ensure that the high frequencies can be filtered off. The peak-to-peak noise that was measured on the Hall Sensor output with no current flowing in the wire was 1.73 mV_{RMS} as shown in Figure 25. As listed in Table 1, the minimum current-limit of 1.5 times the quiescent noise with no field ensures that no false triggers are generated and that reliable current measurements occur at the low end of the range.

$$1.5 \times 1.73 = 2.6\text{-mV}_{RMS} \quad (3)$$

Based on the second-order curve fit shown in Figure 23, the corresponding minimum current is 220 mA.

However, as described in Section 5.1, the accuracy at the low-end of the current is low.

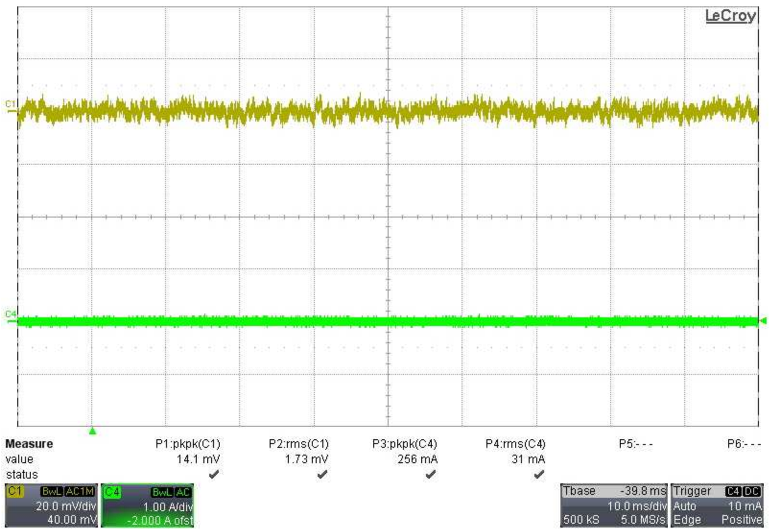

Figure 25. Hall Sensor Output With No current Flowing

5.4 Temperature Data

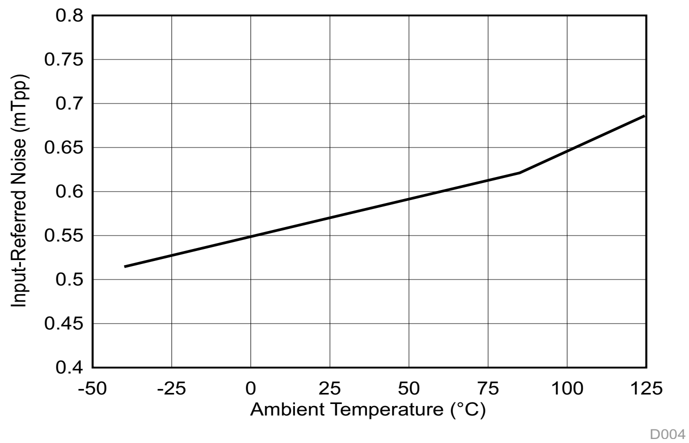

Figure 26. Input Referred Noise vs Ambient Temperature

As shown in Figure 26, a variation of approximately 3.4% occurs from –40°C to 125°C. If the system requires better accuracy over temperature, the on-board temperature sensor, TMP103, can be used to compensate for the variation of temperature versus input-referred noise as shown in Figure 27.

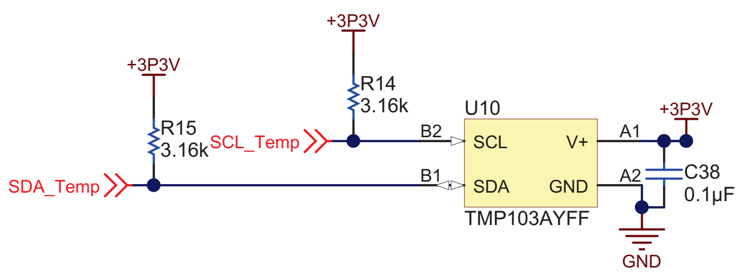

Figure 27. On-Board Temperature Sensor for temperature Compensation

5.5 Life-Time Stress Data (HTOL)

No measurable shift was observed during life time stress of the DRV5053 device.

6 Design Files

6.1 Schematics

The schematics are presented in the following order:

1. MSP430, Hall Sensor (see Figure 28)
2. Power Section, Display (see Figure 29)

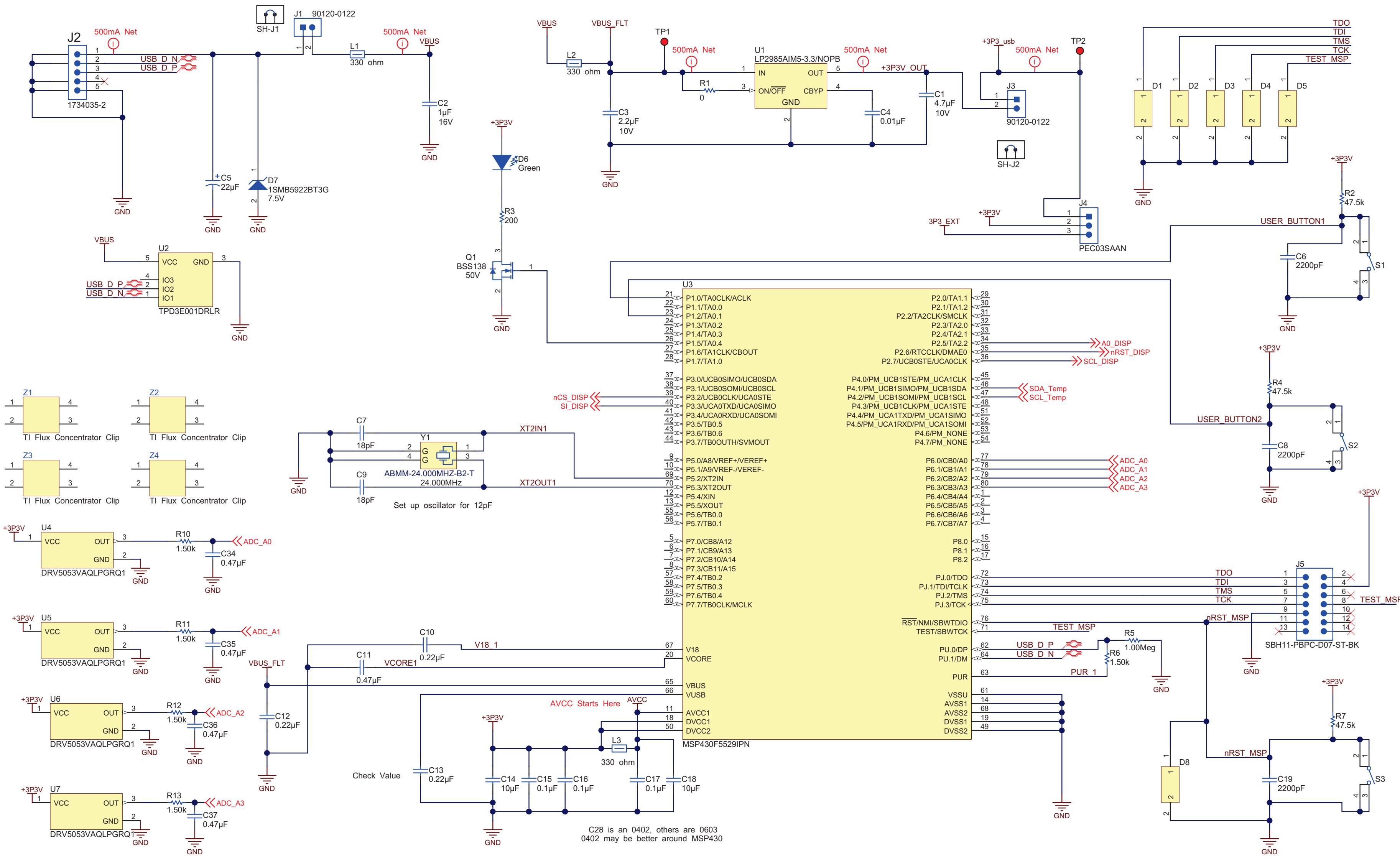

Figure 28. Schematic Section – MSP430, Hall Sensor

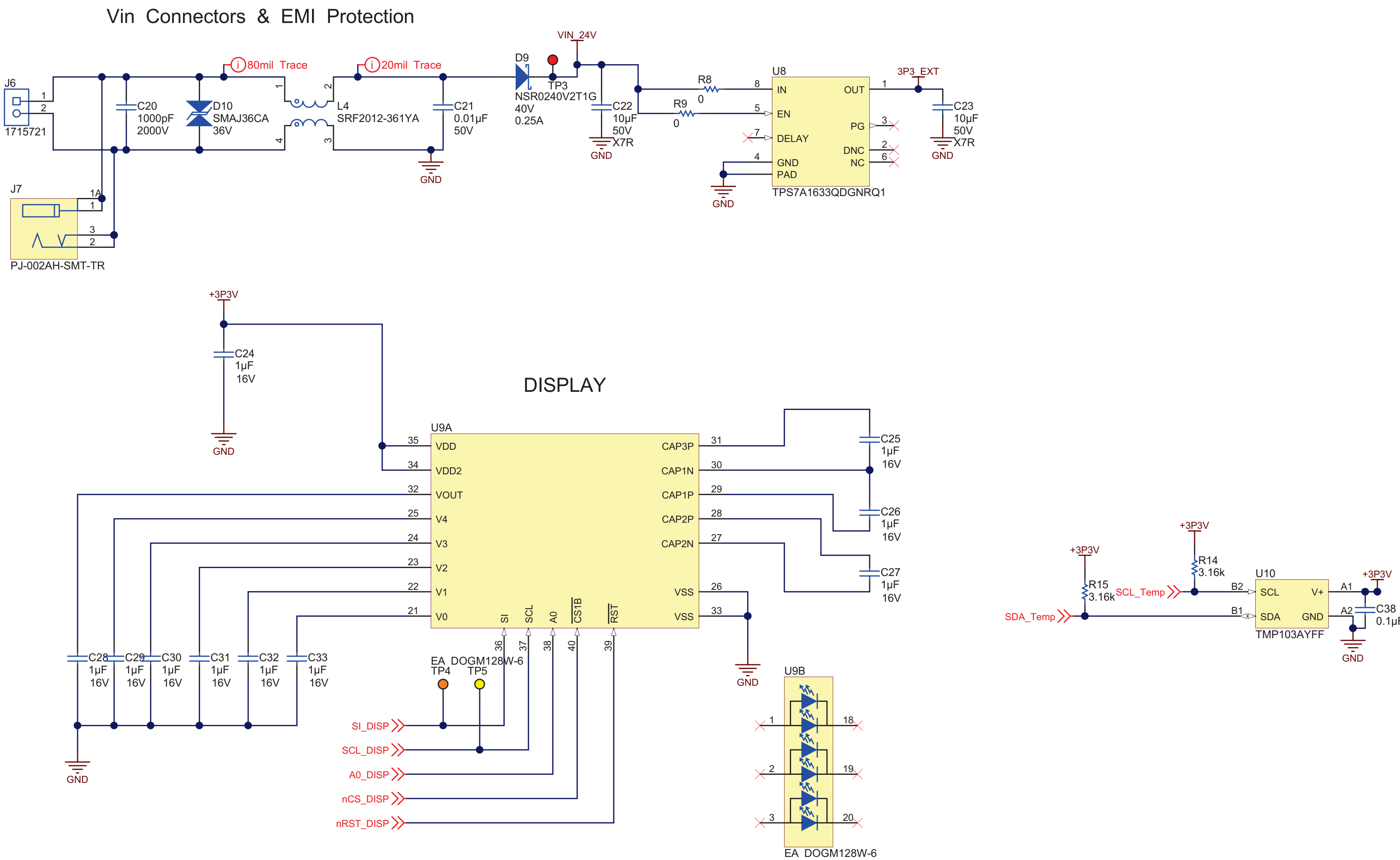

Figure 29. Power Section, Display

6.2 Bill of Materials

To download the bill of materials (BOM), see the design files at TIDA–00218. Table tbd shows the BOM for the Contactless and Precise AC Current Sensing using Hall Sensor Reference Design.

Table 7. BOM

DESIGNATOR	QUANTITY	VALUE	DESCRIPTION	PACKAGE REFERENCE	PART NUMBER	MANUFACTURER
!PCB1	1		Printed Circuit Board		ISE4016	Any
C1	1	4.7µF	CAP, CERM, 4.7µF, 10V, ±10%, X5R, 0805	0805	0805ZD475KAT2A	AVX
C2, C24, C25, C26, C27, C28, C29, C30, C31, C32, C33	11	1µF	CAP, CERM, 1µF, 16V, ±10%, X7R, 0603	0603	C1608X7R1C105K	TDK
C3	1	2.2µF	CAP, CERM, 2.2µF, 10V, ±10%, X5R, 0805	0805	C0805C225K8PACTU	Kemet
C4	1	0.01 µF	CAP, CERM, 0.01 µF, 16V, ±10%, X7R, 0402	0402	GRM155R71C103KA01D	MuRata
C5	1	22µF	CAP ALUM 22UF 10V 20% SMD	E55	EEE–1AA220WR	Panasonic - ECG
C6, C8, C19	3	2200pF	CAP, CERM, 2200pF, 100V, ±5%, X7R, 0603	0603	06031C222JAT2A	AVX
C7, C9	2	18pF	CAP, CERM, 18pF, 50V, ±5%, C0G/NP0, 0603	0603	06035A180JAT2A	AVX
C10, C12, C13	3	0.22µF	CAP, CERM, 0.22µF, 10V, ±10%, X5R, 0402	0402	GRM155R61A224KE19D	MuRata
C11, C34, C35, C36, C37	5	0.47µF	CAP, CERM, 0.47µF, 10V, ±10%, X5R, 0402	0402	GRM155R61A474KE15D	MuRata
C14, C18	2	10µF	CAP, CERM, 10µF, 10V, ±10%, X5R, 0805	0805	C0805C106K8PACTU	Kemet
C15, C16, C38	3	0.1 µF	CAP, CERM, 0.1 µF, 25V, ±5%, X7R, 0603	0603	06033C104JAT2A	AVX
C17	1	0.1 µF	CAP, CERM, 0.1 µF, 16V, ±10%, X5R, 0402	0402	GRM155R61C104KA88D	MuRata
C20	1	1000pF	CAP, CERM, 1000pF, 2000V, ±10%, X7R, 1210	1210	C1210C102KGRACTU	Kemet
C21	1	0.01 µF	CAP, CERM, 0.01 µF, 50V, ±10%, C0G/NP0, 0402	0402	GCM155R71H103KA55D	MuRata
C22, C23	2	10µF	CAP, CERM, 10µF, 50V, ±10%, X7R, 1210	1210	GRM32ER71H106KA12L	MuRata
D1, D2, D3, D4, D5, D8	6		ESD in 0402 Package with 10 pF Capacitance and 6 V Breakdown, 1 Channel, –40 to +125 °C, 2-pin X2SON (DPY), Green (RoHS & no Sb/Br)	DPY0002A	TPD1E10B06DPYR	Texas Instruments
D6	1	Green	LED, Green, SMD	1.6x0.8x0.8mm	LTST-C190GKT	Lite-On
D7	1	7.5V	Diode, Zener, 7.5V, 550mW, SMB	SMB	1SMB5922BT3G	ON Semiconductor
D9	1	40V	Diode, Schottky, 40V, 0.25A, SOD–523	SOD–523	NSR0240V2T1G	ON Semiconductor
D10	1	36V	Diode, TVS, Bi, 36V, 400W, SMA	SMA	SMAJ36CA	Littelfuse
J1, J3	2		Header, 100mil, 2x1, Tin plated, TH	Header 2x1	90120–0122	Molex
J2	1		Connector, Receptacle, Mini-USB Type B, R/A, Top Mount SMT	USB Mini Type B	1734035–2	TE Connectivity
J4	1		Header, 100mil, 3x1, Tin plated, TH	Header, 3 PIN, 100mil, Tin	PEC03SAAN	Sullins Connector Solutions
J5	1		Header (shrouded), 100 mil, 7x2, Gold plated, TH	7x2 Shrouded Header	SBH11-PBPC-D07-ST-BK	Sullins Connector Solutions
J6	1	2x1	Conn Term Block, 2POS, 5.08mm, TH	2POS Terminal Block	1715721	Phoenix Contact
J7	1		Power Jack, SMT	14.8x11x12.6mm	PJ–002AH-SMT-TR	CUI Inc.
L1, L2, L3	3	330 ohm	1.5A Ferrite Bead, 330 ohm @ 100MHz, SMD	0603	BLM18SG331TN1D	MuRata
L4	1		Inductor, Wirewound, Ferrite, , 0.3A, 0.45 ohm, SMD	2.0x1.2x1.2mm	SRF2012–361YA	Bourns

Table 7. BOM (continued)

DESIGNATOR	QUANTITY	VALUE	DESCRIPTION	PACKAGE REFERENCE	PART NUMBER	MANUFACTURER
Q1	1	50V	MOSFET, N-CH, 50V, 0.22A, SOT–23	SOT–23	BSS138	Fairchild Semiconductor
R1	1	0	RES, 0 ohm, 5%, 0.063W, 0402	0402	CRCW04020000Z0ED	Vishay-Dale
R2, R4, R7	3	47.5k	RES, 47.5k ohm, 1%, 0.1W, 0603	0603	CRCW060347K5FKEA	Vishay-Dale
R3	1	200	RES, 200 ohm, 5%, 0.1W, 0603	0603	CRCW0603200RJNEA	Vishay-Dale
R5	1	1.00Meg	RES, 1.00Meg ohm, 1%, 0.063W, 0402	0402	CRCW04021M00FKED	Vishay-Dale
R6	1	1.50k	RES, 1.50k ohm, 1%, 0.063W, 0402	0402	CRCW04021K50FKED	Vishay-Dale
R8, R9	2	0	RES, 0 ohm, 5%, 0.063W, 0402	0402	ERJ–2GE0R00X	Panasonic
R10, R11, R12, R13	4	1.50k	RES, 1.50 k, 1%, 0.063 W, 0402	0402	CRCW04021K50FKED	Vishay-Dale
R14, R15	2	3.16k	RES, 3.16k ohm, 1%, 0.1W, 0603	0603	CRCW06033K16FKEA	Vishay-Dale
S1, S2, S3	3		Switch, Tactile, SPST-NO, 0.05A, 12V, SMT	SW, SPST 6x6 mm	4–1437565–1	TE Connectivity
SH-J1, SH-J2	2	1x2	Shunt, 2mm, Gold plated, Black	2mm Shunt, Closed Top	2SN-BK-G	Samtec
TP1, TP2, TP3	3	Red	Test Point, Miniature, Red, TH	Red Miniature Testpoint	5000	Keystone
TP4	1	Orange	Test Point, Miniature, Orange, TH	Orange Miniature Testpoint	5003	Keystone
TP5	1	Yellow	Test Point, Miniature, Yellow, TH	Yellow Miniature Testpoint	5004	Keystone
U1	1		Micropower 150 mA Low-Noise Ultra Low-Dropout Regulator, 5-pin SOT–23, Pb-Free	MF05A	LP2985AIM5–3.3/NOPB	National Semiconductor
U2	1		Low-Capacitance + / - 15 kV ESD-Protection Array for High-Speed Data Interfaces, 3 Channels, –40 to +85 °C, 5-pin SOT (DRL), Green (RoHS & no Sb/Br)	DRL0005A	TPD3E001DRLR	Texas Instruments
U3	1		Mixed Signal MicroController, PN0080A	PN0080A	MSP430F5529IPN	Texas Instruments
U4, U5, U6, U7	4		Analog Linear Hall –80 mV/mt–40 - 125°C, LPG0003A	LPG0003A	DRV5053VAQLPGRQ1	Texas Instruments
U8	1		60-V, 5-µA IQ, 100-mA, Low-Dropout VOLTAGE REGULATOR With Enable and Power-Good, DGN0008C	DGN0008C	TPS7A1633QDGNRQ1	Texas Instruments
U9	1		Module, 128x64-pixel graphics display	LCD Module	EA DOGM128W–6	Electronic Assembly
U10	1		Low-Power, Digital Temperature Sensor with Two-Wire Interface in WCSP, YFF0004AAAA	YFF0004AAAA	TMP103AYFF	Texas Instruments
Y1	1		Crystal, 24.000MHz, 18pF, SMD	Xtal, 7.2x1.3x5.2mm	ABMM–24.000MHZ-B2-T	Abracon Corportation
Z1, Z2, Z3, Z4	4		TI Flux Concentrator Clip		TI Flux Concentrator Clip	Produkt Works
FID1, FID2, FID3, FID4, FID5, FID6	0		Fiducial mark. There is nothing to buy or mount.	Fiducial	N/A	N/A

6.3 Layer Plots

To download the layer plots, see the design files at TIDA–00218.

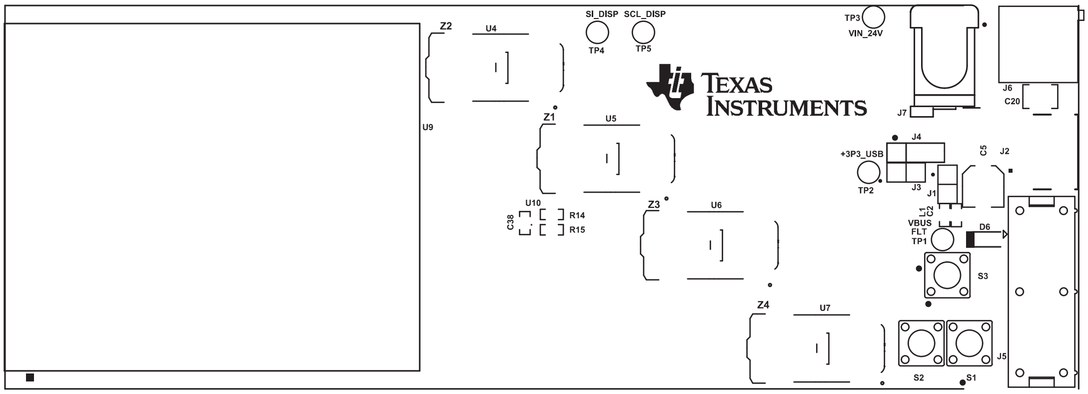

Figure 30. Layer Plot 1

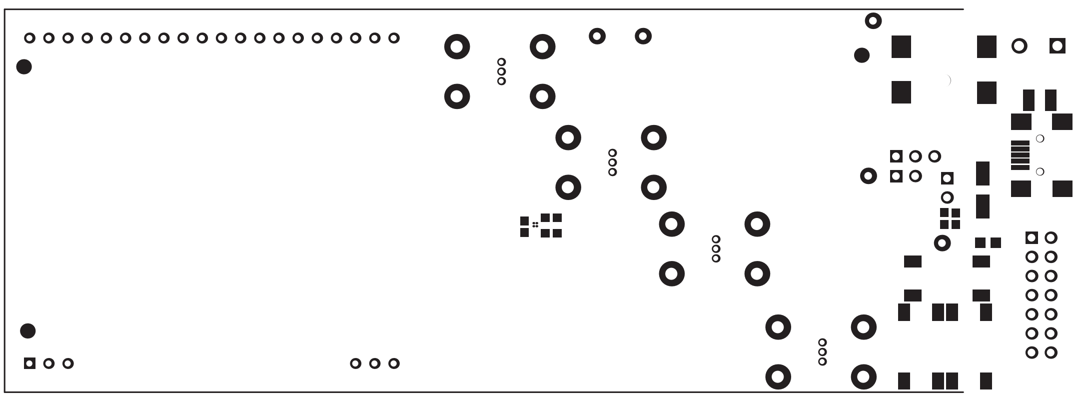

Figure 31. Layer Plot 2

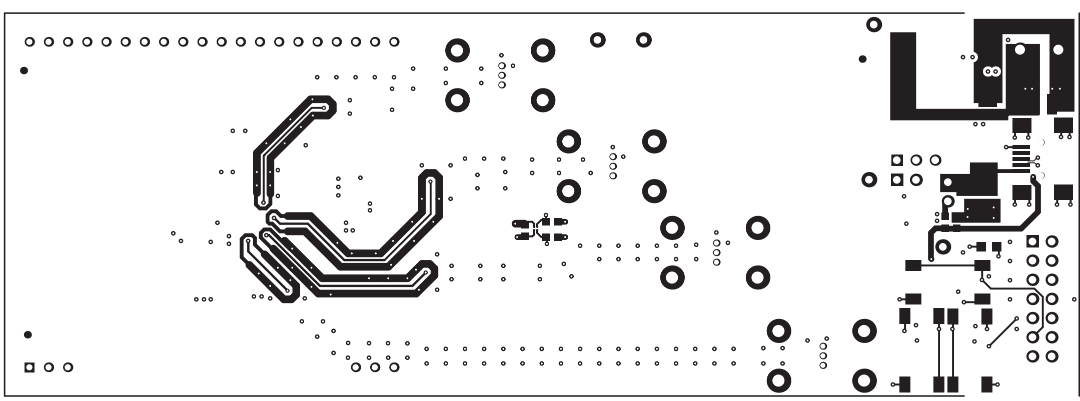

Figure 32. Layer Plot 3

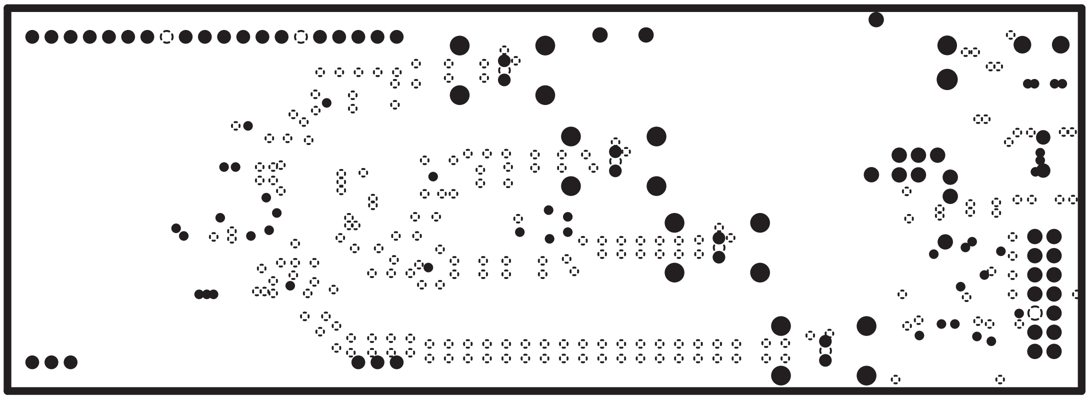

Figure 33. Layer Plot 4

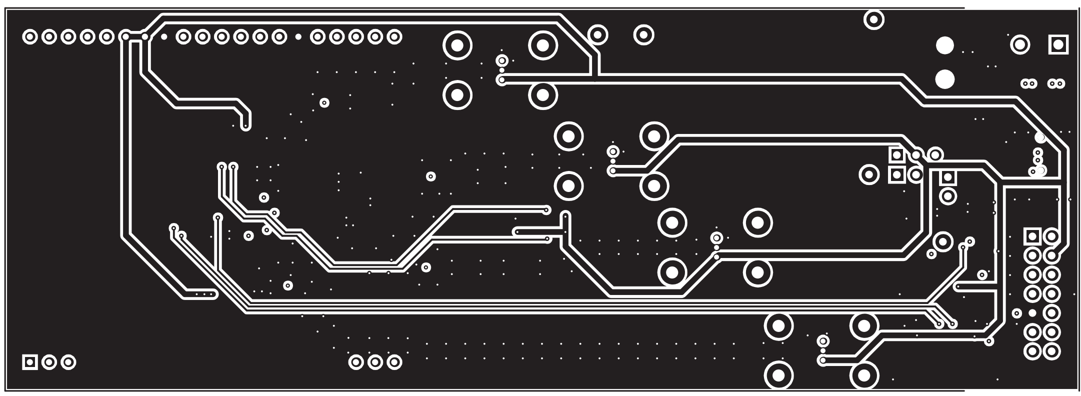

Figure 34. Layer Plot 5

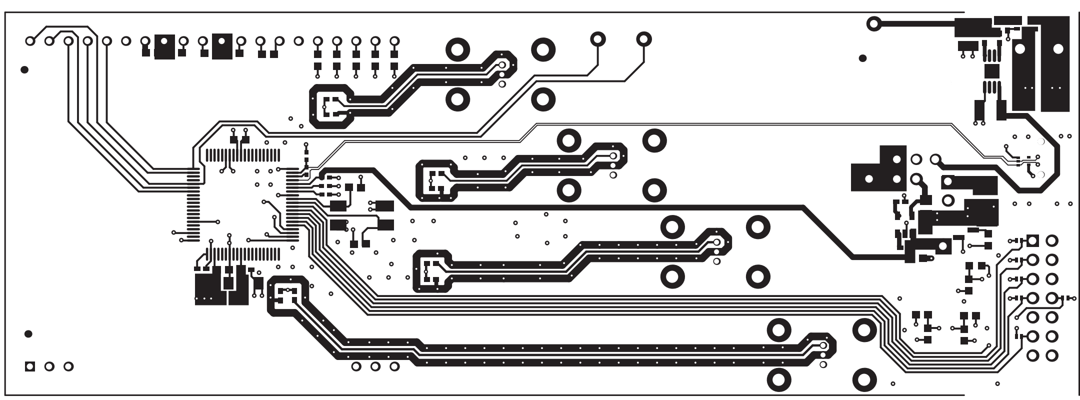

Figure 35. Layer Plot 6

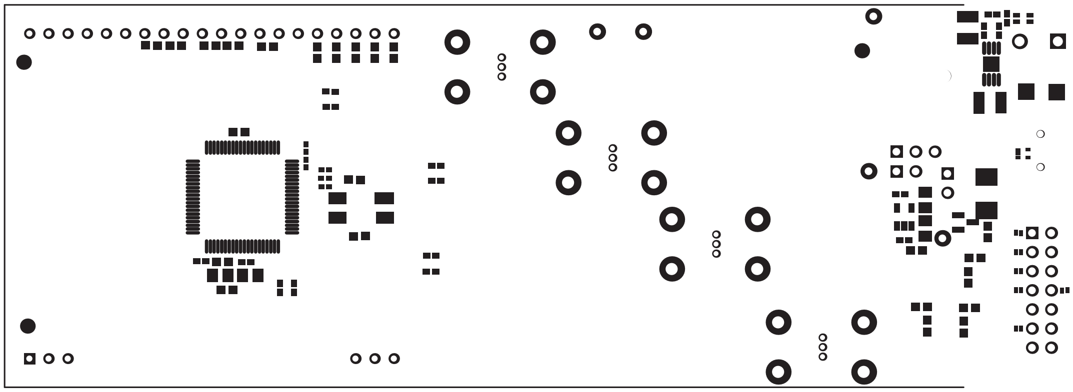

Figure 36. Layer Plot 7

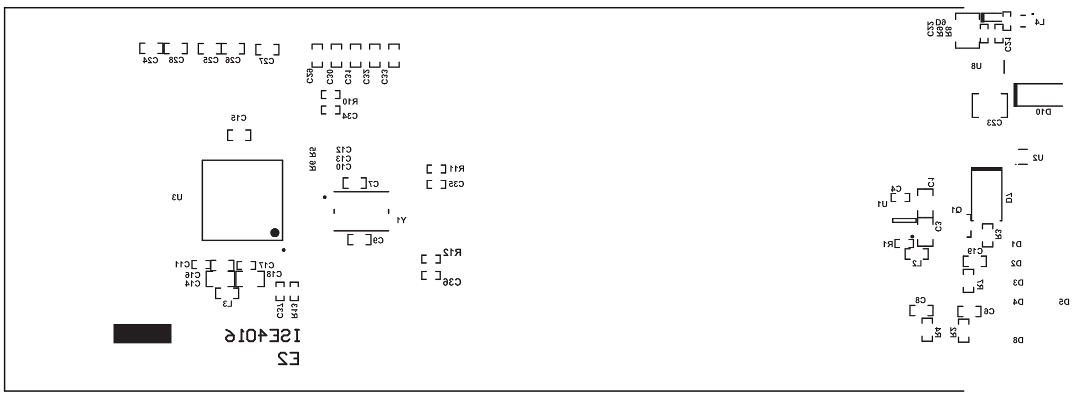

Figure 37. Layer Plot 8

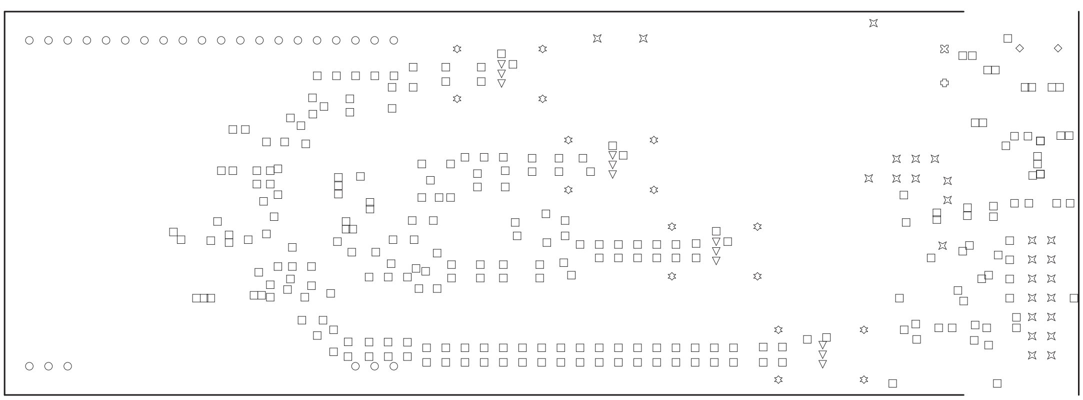

Symbol	Hit Count	Tool Size	Plated	Hole Type
□	250	10mil (0.254mm)	PTH	Round
▽	12	25.984mil (0.66mm)	PTH	Round
○	26	31.496mil (0.8mm)	PTH	Round
□	2	35.433mil (0.9mm)	NPTH	Round
⌑	26	40mil (1.016mm)	PTH	Round
◇	2	51.181mil (1.3mm)	PTH	Round
✡	16	62.992mil (1.6mm)	PTH	Round
☒	1	62.992mil (1.6mm)	NPTH	Round
○	1	70.866mil (1.8mm)	NPTH	Round
	336 Total			

Figure 38. Layer Plot 9

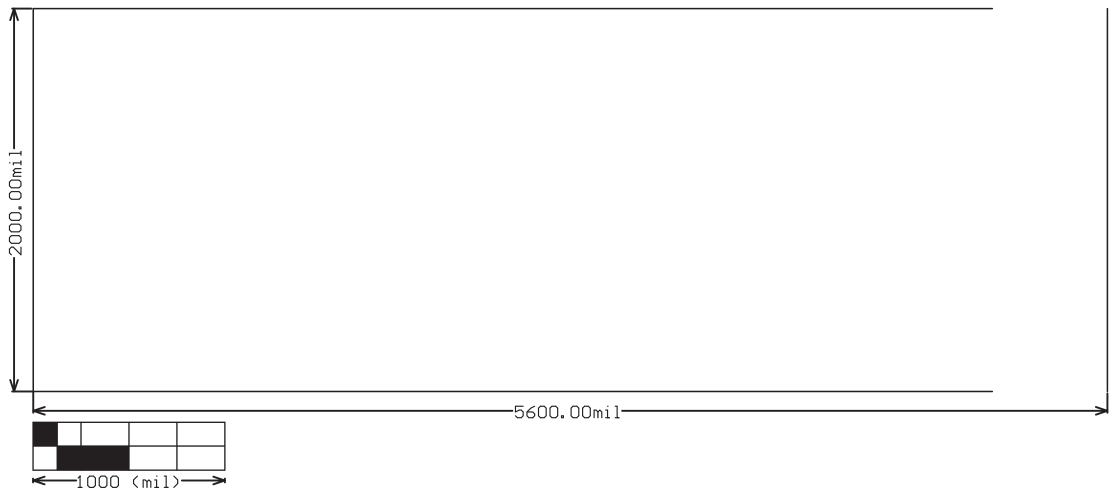

Figure 39. Layer Plot 10

6.4 Altium Project

To download the Altium project files, see the design files at TIDA–00218.

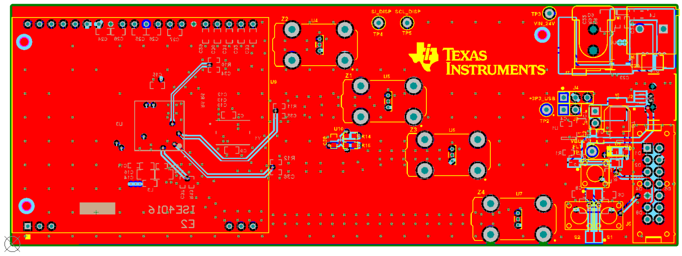

Figure 40. All Layers

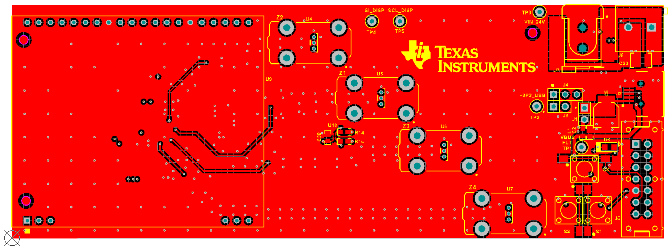

Figure 41. Top Layer

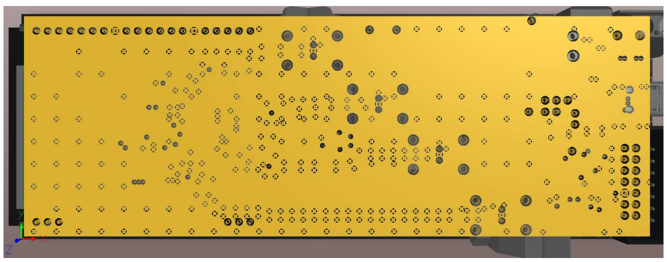

Figure 42. Ground Layer

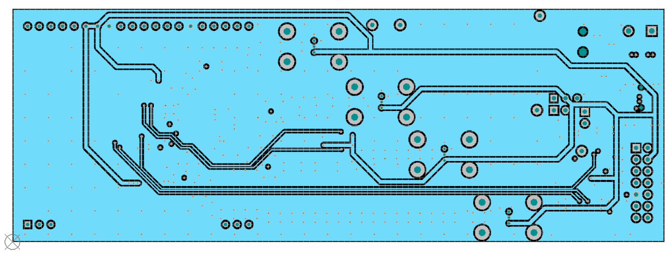

Figure 43. Power Layer

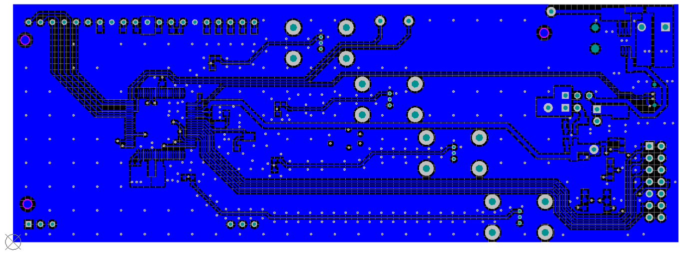

Figure 44. Bottom Layer

6.5 Gerber Files

To download the Gerber files, see the design files at TIDA–00218

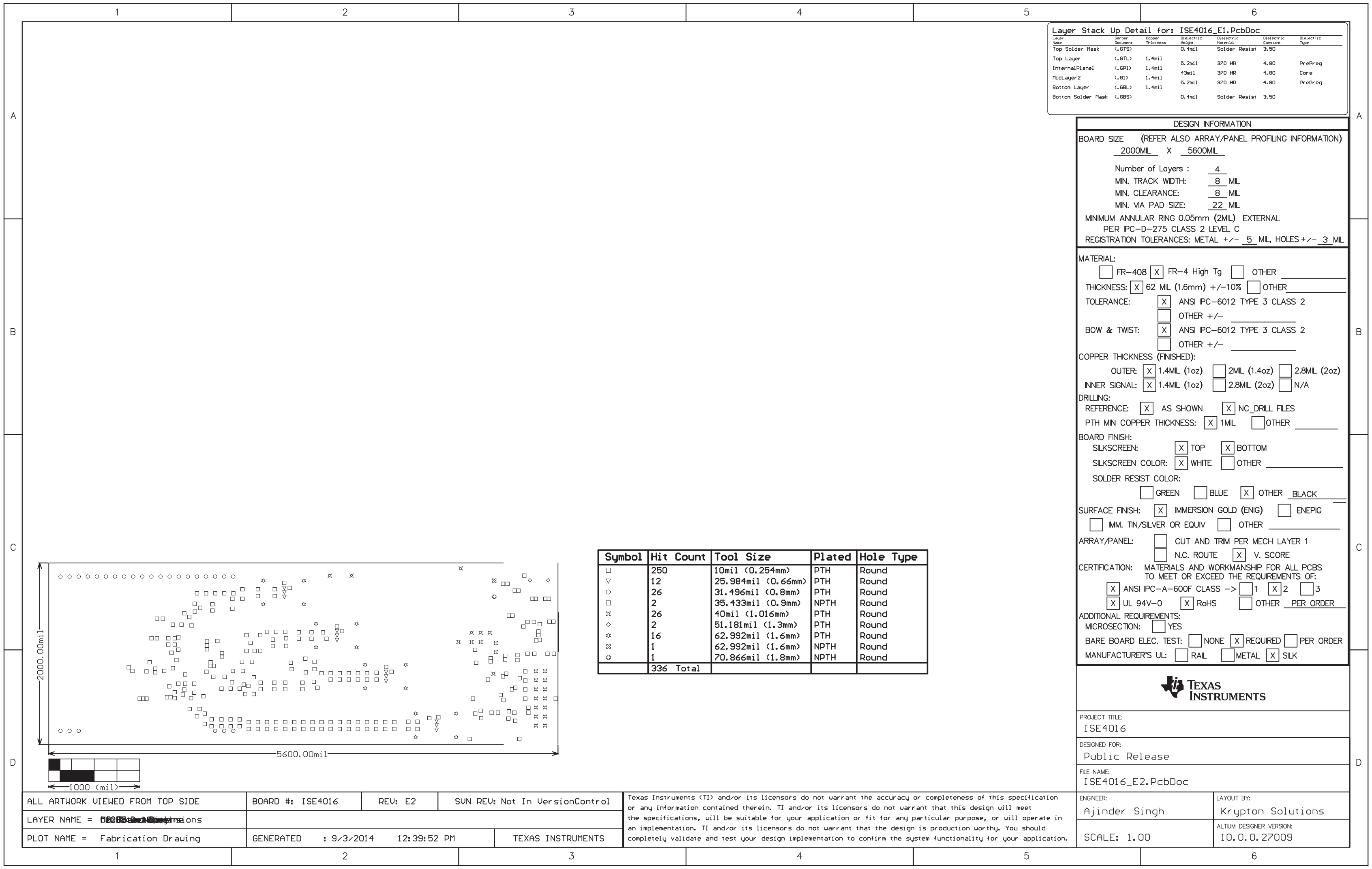

Figure 45. Fabrication Drawing

6.6 Assembly Drawings

ZZ2 ■ These assemblies are ESD sensitive, ESD precautions shall be observed.
ZZ3 ■ These assemblies must be clean and free from flux and all contaminants. Use of no clean flux is not acceptable.
ZZ4 ■ These assemblies must comply with workmanship standards IPC-A-610 Class 2, unless otherwise specified.

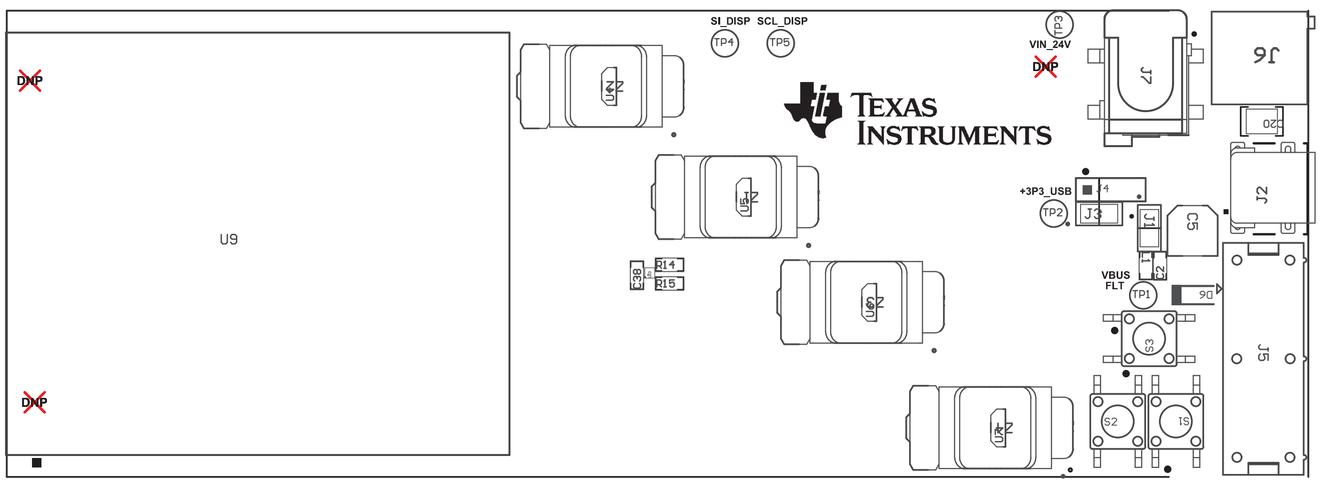

COMPONENTS MARKED 'DNP' SHOULD NOT BE POPULATED.
ASSEMBLY VARIANT: 001

PCB VIEWED FROM TOP SIDE	BOARD #: ISE4016	REV: E2	SVN REV: Not In VersionControl
IGNORE -> Top Overlay			
PLOT NAME = Top Assembly Drawing	GENERATED : 9/3/2014 12:50:45 PM		TEXAS INSTRUMENTS

Figure 46. Assembly Drawing 1

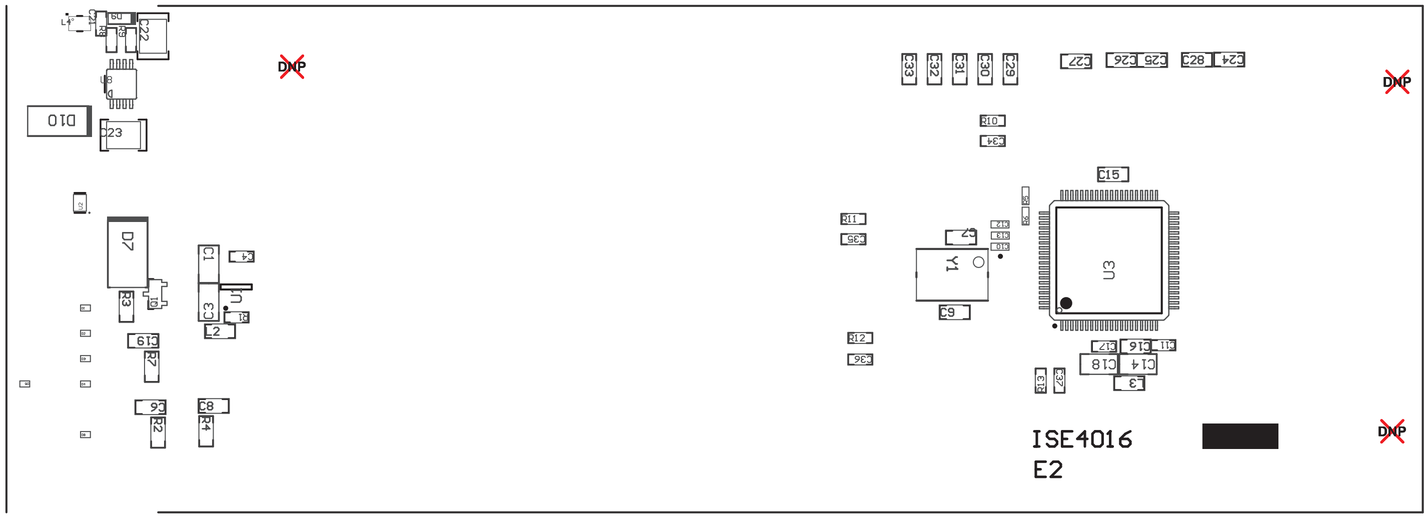

COMPONENTS MARKED 'DNP' SHOULD NOT BE POPULATED.
ASSEMBLY VARIANT: 001

PCB VIEWED FROM BOTTOM SIDE	BOARD #: ISE4016	REV: E2	SVN REV: Not In VersionControl
	IGNORE -> Bottom Overlay		
PLOT NAME = Bottom Assembly Drawing	GENERATED : 9/3/2014 12:50:46 PM		TEXAS INSTRUMENTS

Figure 47. Assembly Drawing 2

6.7 Software Files

To download the software files, see the design files at TIDA–00218

7 References

- *DRV5053 Analog-Bipolar Hall Effect Sensor*, SLIS153
- LP2985–33, *150-mA LOW-NOISE LOW-DROPOUT REGULATOR WITH SHUTDOWN*, SLVS522
- *Magnetic Field of Current*, Magnetic Field of Current
- MSP430F5529, *MIXED SIGNAL MICROCONTROLLER*, SLAS590
- TMP103, *Low-Power, Digital Temperature Sensor with Two-Wire Interface in WCSP*, SBOS545
- TPD3E001, *LOW-CAPACITANCE 3-CHANNEL ±15-kV ESD-PROTECTION ARRAY FOR HIGH-SPEED DATA INTERFACES*, SLLS683
- TPS7A1633, *60-V, 5-μA I_Q100-mA, Low-Dropout Voltage Regulator with Enable and Power-Good*, SBVS171

8 About the Author

AJINDER PAL SINGH is a Systems Architect at Texas Instruments, where he is responsible for developing reference design solutions for the industrial segment. Ajinder brings to this role his extensive experience in high-speed digital, low-noise analog and RF system-level design expertise. Ajinder earned his Master of Science in Electrical Engineering (MSEE) from Texas Tech University in Lubbock, TX. Ajinder is a member of the Institute of Electrical and Electronics Engineers (IEEE).

MARK C. DAHLMAN, P.E. is an Analog Field Applications Engineer at Texas Instruments, Incorporated where he supports analog products in the South Eastern United States region. Mark has 18+ years of design and applications experience, specializing in power systems, power electronics, data conversion, high speed interface, industrial interface, automotive systems, and audio systems. Mark earned his Bachelor of Science in Electrical Engineering (BSEE) from Tennessee Technological University in 1996 and received his Professional Engineering License in 2003. Mark is a member of the Institute of Electrical and Electronics Engineers (IEEE).

Revision History

Changes from Original (October 2014) to A Revision	Page
• Added "Control Panel" to Featured Applications	1
• Updated device status to production data	6

NOTE: Page numbers for previous revisions may differ from page numbers in the current version.

Mailing Address: Texas Instruments, Post Office Box 655303, Dallas, Texas 75265